Marine Environmental Research 189 (2023) 106046

Contents lists available at ScienceDirect

Marine Environmental Research

journal homepage: www.elsevier.com/locate/marenvrev

Seafloor warm water temperature anomalies impact benthic macrofauna communities of a high-Arctic cold-water fjord

Èric Jordà-Molina [a,*], Paul E. Renaud [b,c], Marc J. Silberberger [d], Arunima Sen [a,c], Bodil A. Bluhm [e], Michael L. Carroll [b], William G. Ambrose Jr. [f], Finlo Cottier [g,e], Henning Reiss [a]

[a] Nord University, Faculty of Biosciences and Aquaculture, 8049, Bodø, Norway
[b] Akvaplan-niva, Fram Centre for Climate and Environment, N-9296, Tromsø, Norway
[c] University Centre in Svalbard (UNIS), Longyearbyen, N-9170, Norway
[d] Institute of Oceanology Polish Academy of Sciences, Powstańców Warszawy 55, 81-712, Sopot, Poland
[e] UiT – the Arctic University of Norway, N-9037, Tromsø, Norway
[f] Office of Polar Programs, Antarctic Organisms and Ecosystems, National Science Foundation, 2415 Eisenhower Ave, Alexandria, Virginia, 22314, USA
[g] Scottish Association for Marine Science, Oban, Argyll, PA37 1QA, UK

ARTICLE INFO

Keywords:
Arctic
Benthic communities
Marine heatwaves (MHWs)
Fjord
Coastal environment
Community change
Time series
Ecosystem disturbance

ABSTRACT

Amid the alarming atmospheric and oceanic warming rates taking place in the Arctic, western fjords around the Svalbard archipelago are experiencing an increased frequency of warm water intrusions in recent decades, causing ecological shifts in their ecosystems. However, hardly anything is known about their potential impacts on the until recently considered stable and colder northern fjords. We analyzed macrobenthic fauna from four locations in Rijpfjorden (a high-Arctic fjord in the north of Svalbard) along its axis, sampled intermittently in the years 2003, 2007, 2010, 2013 and 2017. After a strong seafloor warm water temperature anomaly (SfWWTA) in 2006, the abundance of individuals and species richness dropped significantly across the entire fjord in 2007, together with diversity declines at the outer parts (reflected in Shannon index drops) and increases in beta diversity between inner and outer parts of the fjord. After a period of three years with stable water temperatures and higher sea-ice cover, communities recovered through recolonization processes by 2010, leading to homogenization in community composition across the fjord and less beta diversity. For the last two periods (2010-2013 and 2013-2017), beta diversity between the inner and outer parts gradually increased again, and both the inner and outer sites started to re-assemble in different directions. A few taxa began to dominate the fjord from 2010 onwards at the outer parts, translating into evenness and diversity drops. The inner basin, however, although experiencing strong shifts in abundances, was partially protected by a fjordic sill from impacts of these temperature anomalies and remained comparatively more stable regarding community diversity after the disturbance event. Our results indicate that although shifts in abundances were behind important spatio-temporal community fluctuations, beta diversity variations were also driven by the occurrence-based macrofauna data, suggesting an important role of rare taxa. This is the first multidecadal time series of soft-bottom macrobenthic communities for a high-Arctic fjord, indicating that potential periodic marine heatwaves might drive shifts in community structure, either through direct effects from thermal stress on the communities or through changes in environmental regimes led by temperature fluctuations (i.e. sea ice cover and glacial runoff, which could lead to shifts in primary production and food supply to the benthos). Although high-Arctic macrobenthic communities might be resilient to some extent, sustained warm water anomalies could lead to permanent changes in cold-water fjordic benthic systems.

Abbreviations: SfWWTA, Seafloor Warm Water Temperature Anomaly; MHW, Marine Heatwave; AW, Atlantic Water; ArW, Arctic Water; AO, Arctic Oscillation Index; LCBD, Local Contribution to Betadiversity; AEMs, Assimetric Eigenvector Maps; TBI, Temporal Beta diversity Index.

* Corresponding author.
E-mail address: eric.jorda-molina@nord.no (È. Jordà-Molina).

https://doi.org/10.1016/j.marenvres.2023.106046
Received 24 April 2023; Received in revised form 29 May 2023; Accepted 3 June 2023
Available online 5 June 2023

1. Introduction

Arctic air temperatures have warmed more than four times faster in the last four decades than in other parts of the globe (Rantanen et al., 2022). In particular, the warming rate for the Northern Barents Sea region is five to seven times the global averages and this exceptional heating is strongly linked to large reductions in sea ice concentration and increased sea surface temperatures in this "warming hotspot" (Isaksen et al., 2022). In light of this rapid change, long-term monitoring programs of the marine Arctic ecosystem are urgently needed in order to establish baselines and rates of environmental change to disentangle short-term variation from long-term shifts, and to predict future scenarios relevant to management efforts. Benthic community structure and function are determined by environmental drivers and faunal interactions over multiple temporal and spatial scales (Griffiths et al., 2017; Ehrnsten et al., 2020). By integrating the variability of these processes into their structure, benthic communities (which are mainly sessile and long-lived) have been proposed as excellent sentinels of environmental change (Renaud et al., 2008; Carroll et al., 2011). Their community fluctuations can thus indicate climate- or other human-driven changes (e.g., Kröncke et al., 1998; Larkin et al., 2010; Serrano et al., 2022).

In shelf and coastal areas, macrobenthic communities play crucial roles in carbon cycling and the remineralization of nutrients (Bourgeois et al., 2017; Solan et al., 2020). Particularly, fjords, which are common geomorphological features in high and mid-latitude regions, are regarded as important carbon sinks on a global scale (Smith et al., 2015; Faust and Knies, 2019; Włodarska-Kowalczuk et al., 2019). These semi-enclosed estuaries experience high seasonality in primary production and strong gradients in abiotic parameters such as salinity, temperature, oxygen concentrations, sedimentation rates, supply of nutrients, and organic matter concentration in the sediments that cause gradients of benthic assemblages along the fjord axis (Holte and Gulliksen, 1998; Włodarska-Kowalczuk et al., 1998; Włodarska-Kowalczuk et al., 2005; Jordà Molina et al., 2019; Udalov et al., 2021).

Isolation caused by fjordic sills in Arctic fjords may protect inner-basin communities from strong fluctuations of abiotic factors occurring in off-shore shelf regions and, therefore, such fjords are assumed to act as refugia (Renaud et al., 2007; Kędra et al., 2010; Wesławski et al., 2011). Consequently, inner-fjord benthic communities are not just subsets of the species pools present in adjacent shelves but, in fact, they rather differ in species composition, species richness, diversity, functional complexity and redundancy (Włodarska-Kowalczuk et al., 2012; Udalov et al., 2021). Therefore, benthic communities from Arctic inner-fjord basins could be less resilient to species losses or invasions, and the extent of environmental variation that these communities can tolerate remains unclear in case of extreme disturbance events (Włodarska-Kowalczuk et al., 2012).

The waters around the Svalbard archipelago comprise a transitional domain from warm and salty Atlantic Waters (AW) dominating the south and west of the archipelago, to colder and less saline Arctic Waters (ArW) mainly present in the northern and eastern regions. In recent decades, a progression of the AW over the ArW domain has been observed, a phenomenon that has been termed Atlantification of the Arctic (Polyakov et al., 2020; Ingvaldsen et al., 2021; Tsubouchi et al., 2021). Periodic intrusions of AW into the western Svalbard shelf and the adjacent fjords have been increasingly frequent in the last two decades, especially after 2011 (Bloshkina et al., 2021). Similarly, a time series in the northern waters of the shelf and shelf-break of Svalbard showed that after 2011, previous stable conditions with high ice cover, below 0 °C water temperatures in the upper 50 m and shallow mixing layer depths shifted towards more open-water conditions, persistent shallow water temperatures above 0 °C and large interannual variations in mixing layer depths and ocean-to-atmosphere heat fluxes (including observations of extreme winter conditions with exceptional deep mixing layer depths) (Athanase et al., 2020). In north-eastern fjords of the archipelago, abundant sea ice cover during the early 2000's was followed by a decrease in winter sea-ice cover after 2010, with strong links to increased surface air temperatures (Dahlke et al., 2020). In addition, marine heatwaves (MHWs), characterized as prolonged discrete anomalously warm water events (Hobday et al., 2016), have been increasingly recorded in the Barents Sea and in the Fram Strait throughout the last two decades (Beszczynska-Möller et al., 2012; Mohamed et al., 2022).

The impacts of this ongoing Atlantification and extreme warming events of the waters around Svalbard are not limited to hydrography, but also to shifts in the structure and function of their ecosystems (Wassmann et al., 2011; Ingvaldsen et al., 2021). With increased ocean temperatures, the ranges of many boreal species are expected to expand northward (Kraft et al., 2013; Renaud et al., 2015, 2019). In the Barents Sea, several studies have already documented an increase in the presence of boreal fish, zooplankton, and benthic species (Dalpadado et al., 2012; Kortsch et al., 2012; Fossheim et al., 2015). This poleward expansion of boreal species may alter the intrinsic functionality of receiving communities (Kortsch et al., 2012; Węsławski et al., 2017; Renaud et al., 2019; Csapó et al., 2021). Thermal stress induced by unusual warm water temperature events (temperature anomalies such as MHWs) can have detrimental consequences for benthic communities when exceeding species thermal ranges (Dolbeth et al., 2021), inducing mass mortality events in severe cases (Hobday et al., 2016; Garrabou et al., 2022) or shifts in species abundances and/or biomass (Pansch et al., 2018). At the same time, when not lethal, thermal stress may lead to behavioral changes in benthic organisms affecting, for instance, bioturbation activities (Kauppi et al., 2023). However, indirect responses can also be mediated by changes in other biotic interactions "post-disturbance" (Pansch et al., 2018). For instance, ocean temperature fluctuations in Arctic fjords can simultaneously lead to shifts in other important environmental variables that constrain benthic community structure and function (e.g. sea ice cover with consequent shifts in primary production, qualitative and quantitative food availability at the seafloor, water mass properties and glacier runoff and turbidity) (Wesławski et al., 2011). Therefore, the extreme complexity of interactions in the natural environment driven from temperature shifts and its effects on biological communities should be taken into account.

The western and southern fjords of Svalbard have been extensively studied (Molis et al., 2019). Carroll and Ambrose (2012) first reported on macrofaunal patterns on the shelf and fjords of northeastern Svalbard in 2003 in relation to Atlantic and Arctic water masses. Although changes in sea ice and oceanographic regimes have been documented in northern Svalbard during the last two decades (Athanase et al., 2020; Dahlke et al., 2020), no long-term monitoring studies exist of benthic fauna for this area.

Here, we analyze an intermittent time series (from 2003 to 2017) of the soft-bottom macrobenthic communities from Rijpfjorden, a fjord located on the northern coast of the Svalbard archipelago. Although this has historically been considered a fjord with predominantly Arctic conditions, periodic intrusions of warm Atlantic waters from the continental slope have been reported to protrude into the shelf area, affecting the physico-chemical setting and the pelagic ecosystem surrounding this fjord (Hop et al., 2019). Although no significant sustained warming trends have been found throughout the last decades in Rijpfjorden (Cottier et al., 2022), a long-term mooring deployed at the mid-region of the fjord since 2006 provides indications of seafloor warm water temperature anomalies (SfWWTAs) throughout the last decades, which we report in the present article.

Our study investigates how these periodic SfWWTAs in the historically ArW-influenced Rijpfjorden might have affected the temporal dynamics of macrofauna communities. We hypothesize that the species composition in years preceded by SfWWTAs will differ from those preceded by more stable and cold-water periods. We then put the interannual changes in community composition into the spatial context along the fjord axis and hypothesize that outer stations, which are more exposed to the continental shelf and therefore more directly influenced

by the effects of potential warm Atlantic inflows from the slope, will show larger inter-annual fluctuations than communities inhabiting the inner silled basin. We also investigate whether bottom temperature fluctuations (i.e. anomalies) by themselves can drive community shifts and if other environmental variables known to be important for benthic community structure in Arctic fjords (which can be simultaneously impacted by temperature, such as sea ice cover and glacier runoff) can also have an impact on macrofauna compositional change. Once again, we hypothesize that at outer stations, fluctuations in temperature will have a stronger influence in determining community composition through time, while more protected inner locations will be less directly influenced by bottom water temperature.

2. Materials and methods

2.1. Study area

Rijpfjorden is located on the northern coast of the Nordaustlandet island, in the north-east of the Svalbard archipelago (Fig. 1a). This fjord is ca. 40 km long and between 7 and 13 km wide. The fjord opens into a wide bay which connects it to the shelf north of Svalbard (100–200 m water depth) which leads to the shelf-break of the Arctic Ocean. The fjord has an inner basin with a maximum water depth of 215 m and an outer basin with 290 m water depth. These two basins are separated by a sill, crossing the fjord diagonally in a northwest-southeast direction, with water depths ranging from ca. 50 m–140 m (Fig. 1d).

Rijpfjorden faces towards the Arctic Ocean and is mainly influenced by comparatively cold and fresh ArW (Hop et al., 2019) with surface temperatures close to the freezing point for most of the year (Wang et al., 2013). AW, however, occasionally penetrates into the shelf area surrounding the fjord (Hop et al., 2019; Wallace et al., 2010). These intrusions are influenced by topographic features of the submarine landscape (troughs and banks along the shelf break) (Bluhm et al., 2020) and also by the wind patterns prevailing in the area (Onarheim et al., 2014; Kolås et al., 2020).

Sea ice usually covers the fjord for up to 9 months a year (Ambrose et al., 2006; Leu et al., 2011) although sea ice extent and volume have been variable during the last decade, with a minimum in 2013 (Hop et al., 2019), and shorter fjord ice seasons have been attributed to reduced sea ice north-east of Svalbard and increased water temperatures (Johansson et al., 2020). Two marine-terminating glaciers are located in the western part of the fjord (Fig. 1c).

2.2. Sampling and macrofauna processing

Sampling took place in 2003, 2007, 2010, 2013 and 2017 with the research vessels *Lance* and *Helmer Hanssen* between late July and early September. Four stations along a transect were studied in the time-series: 'Inner Rijpfjorden' (**IR**) in the inner basin, 'Middle Rijpfjorden' (**MR**) in the outer basin, 'Outer Rijpfjorden' (**OR**) at the fjord mouth located in a depression outside of the outer basin, and 'Rijpfjorden North' (**RN**) just north of the fjord, on the shallow shelf (Table 1; Fig. 1c and d). Stations IR and OR were sampled in all sampled events, station RN in four years and MR in two years (Table 1).

At each station, three Van Veen grab samples of 0.1 m^2 each were retrieved and sediment was sieved over a 0.5 mm mesh. Fauna collected were preserved in a 4% buffered formaldehyde and Rose Bengal stain. In the lab, macrofauna was sorted under the stereomicroscope and identified to the lowest taxonomic level possible. Taxonomic names were checked using the World Register of Marine Species (WoRMS) (Worms Editorial Board, 2022).

2.3. Environmental data

Mean daily water temperatures between 2006 and 2019 from 200 m depth were retrieved from a mooring system located close to station MR (80.3N; 022.3E). From these, the temperature climatology of the bottom water was calculated by averaging data over all the years for each day of the year. Periods of time when mean temperatures exceeded the 90th percentile of the climatology and which lasted for more than five consecutive days were defined as periods with MHWs, following the definition of Marine Heatwaves (MHWs) by Hobday et al. (2016), but with climatology calculated from the 14 years of available mooring data instead of 30 years. Since we calculated climatology based on 14 years of available data in contrast to the recommended 30 years, our MHW definitions should be regarded with caution and just as indicative of temperature anomalies that could potentially be considered MHWs. Therefore, we refer to these as seafloor warm water temperature anomalies (SfWWTAs) in our study.

CTD casts were used to retrieve temperature and salinity profiles close to each station during events of macrofauna sampling. However, for some stations/years some CTD casts were missing, and we retrieved the closest CTD casts in space and time to the sampling points from the UNIS hydrographic database (Skogseth et al., 2019).

Monthly mean Arctic Oscillation indices (AO) were retrieved from the National Weather Service of NOAA,[1] and the average of the year prior to each macrofauna sampling event was calculated to include in constrained analysis of environmental drivers on macrofauna. Some studies suggest that higher inflows of Atlantic water into the Arctic Ocean could be consistent with the positive phase of the AO (Ślubowska et al., 2005), a climate index that describes the patterns in atmospheric circulation over the Arctic. In its negative phase, the polar vortex over the Arctic gets weaker, allowing cold air to escape towards lower latitudes while the westerly winds in the Arctic region fade (Rigor et al., 2002). The opposite occurs during the positive phase, when the polar vortex strengthens and cold air and lower pressures are kept in the Arctic.

In high Arctic fjords, such as Kongsfjorden, it has been postulated that the sedimentation gradient caused by glacial runoff is one of the main drivers of macrofauna composition along the fjordic axis (Włodarska-Kowalczuk et al., 2005; Udalov et al., 2021). Glacial input into Rijpfjorden is not substantial relative to other Svalbard fjords (Santos-Garcia et al., 2022), but may have local influence on the inner fjord station. Therefore, daily glacial runoff simulations ($m^3\ s^{-1}$) based on the simulations by van Pelt et al. (2019) were computed using surface topography and ice thickness to derive the equipotential surface (Torsvik et al., 2019). These data were provided by the Norwegian Polar Institute (Jack Kohler, personal communication) for four locations around the discharge area of the marine-terminating glacier Rijpbreen available from 2006 to 2019 (Fig. 1c). The daily average runoff for all discharge stations was calculated and then the average runoff from the previous year before each macrofauna sampling event was calculated to use as constraining variables for the macrofauna variation partition.

Granulometry analysis and the assessment of Total Organic Carbon content (TOC) in the sediments were conducted for the years 2003 and 2010 taken from an extra grab sample. Granulometry samples were split into coarse (>0.063 mm) and fine fractions (<0.063 mm) by wet sieving and dried at 60 °C and weighted (Carroll and Ambrose, 2012). For TOC content analysis, samples were treated with hydrochloric acid (HCl) to eliminate carbonates and posteriorly, samples were burned at 480 °C in a Leco IR 212 carbon analyzer (Carroll and Ambrose, 2012). Finally, the CO_2 content from the liberated gas was converted to %TOC (Nelson and Sommers, 1996).

A time series of sea ice categories at each station was retrieved from an ice chart repository courtesy of Ice Service at the Norwegian Meteorological Institute, Tromsø, Norway (Nick Hughes, personal communication). The Ice Service classifies sea ice into six categories based on the type of ice and its concentration (out of 10) according to the World

[1] https://www.cpc.ncep.noaa.gov/products/precip/CWlink/daily_ao_index/ao.shtml; accessed the 09.09.2022.

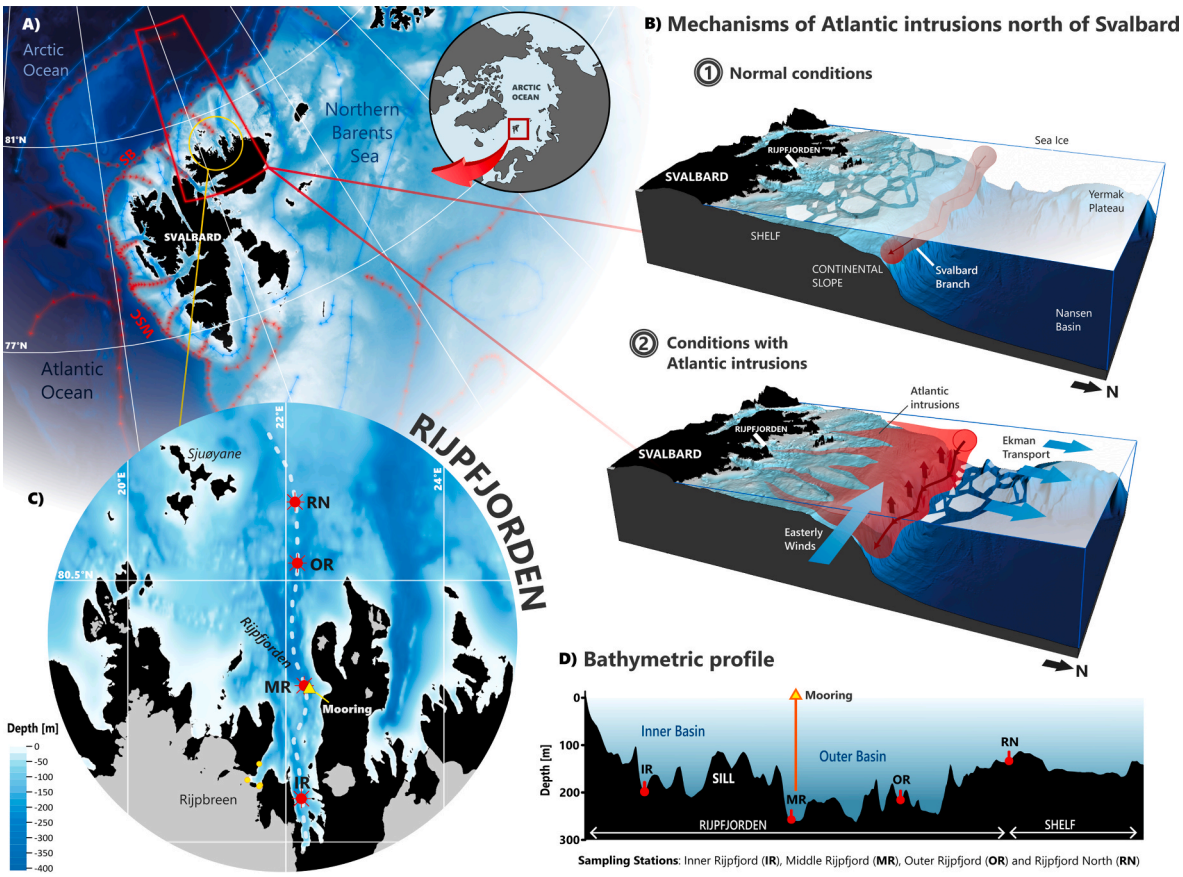

Fig. 1. Study area. **a)** An overview of the Svalbard archipelago with the main currents (red arrows indicate warm Atlantic waters and blue arrows indicate colder Arctic waters; Vihtakari, 2020) and bathymetry. WSC=West Spitsbergen Current; SB=Svalbard Branch. **b)** Mechanisms of Atlantic intrusions in the area north of Svalbard and in the area around Rijpfjorden (red polygon); **1**, during normal conditions without Atlantic instrusions, the Svalbard branch flows along the continental slope and sea ice cover is usually high in the area. **2**, when easterly winds prevail in the area, the Ekman transport generated pushes the drifting sea ice northwards, lifting the Svalbard branch and protruding into the shelf area. **c)** Map of Rijpfjorden (indicated by the yellow circle in map a)) showing the macrofauna sampling locations (IR=Inner Rijpfjorden; MR = Middle Rijpfjorden; OR=Outer Rijpfjorden and RN=Rijpfjorden North) shown with red dots. Yellow triangle indicates the location of the long-term mooring system. Yellow dots indicate the coordinates for glacial runoff simulations of Rijpbreen. Land is indicated in black and glaciers are in grey. **d)** Bathymetric profile along the fjord axis (indicated with white dashed line in map c)), including the location of the four stations with their respective water depths and approximate location of the mooring system. Bathymetry data source: GEBCO Compilation Group (2022)

Table 1
Sampling years, coordinates (latitude and longitude), water depth and average bottom water temperature and salinity over the years sampled from CTD casts (standard deviation (±) and range of minimum and maximum values are indicated). Total organic carbon content (TOC (%)) and grain size fraction <0.063 μm (%) of the 0–2 cm sediment layer only for years 2003 and 2010 are indicated as super index A and B respectively.

Station	Sampled years	Latitude °N	Longitude °E	Depth [m]	Bottom Temperature [°C]	Bottom Salinity	TOC (%)	Grain size fraction <0.063 μm (%)
IR (Inner Rijpfjorden)	*2003, 2007, 2010, 2013, 2017*	80.083	22.195	205	−1.78 ± 0.12 (-1.87; −1.63)	34.74 ± 0.12 (34.61; 34.90)	1.19^{A} 1.35^{B}	$91,9^{A}$ 93^{B}
MR (Middle Rijpfjorden)	*2007, 2010*	80.299	22.233	250	−1.71 ± 0.06 (-1.75; −1.66)	34.68 ± 0.07 (34.63; 34.72)	1.45^{B}	$83,3^{B}$
OR (Outer Rijpfjorden)	*2003, 2007, 2010, 2013, 2017*	80.533	22.146	230	−1.36 ± 0.54 (-1.82; −0.54)	34.69 ± 0.13 (34.59; 34.90)	1.44^{A} 1.66^{B}	$97,6^{A}$ $94,2^{B}$
RN (Rijpfjorden North)	*2007, 2010, 2013, 2017*	80.650	22.115	130	0.37 ± 1.60 (-0.56; 2.75)	34.72 ± 0.15 (34.59; 34.90)	1.48^{B}	90^{B}

Meteorological Organization (WMO) Ice Chart Colour Code Standard (WMO/TD-No. 1215) and Sea Ice Nomenclature (WMO-259): Fast Ice (10/10th), Very Close Drift Ice (9–10/10ths), Close Drift Ice (7–9/10ths), Open Drift Ice (4–7/10ths), Very Open Drift Ice (1–4/10ths) and Open Water (0–1/10ths). Using qGIS (QGIS.org, 2022), the polygons for each ice type was retrieved daily from 2003 to 2018 at each sampling station (Fig. 2f).

2.4. Analysis of inter-annual fluctuations in macrofauna composition

2.4.1. Alpha-diversity

Alpha-diversity indices (species richness (S), Shannon diversity

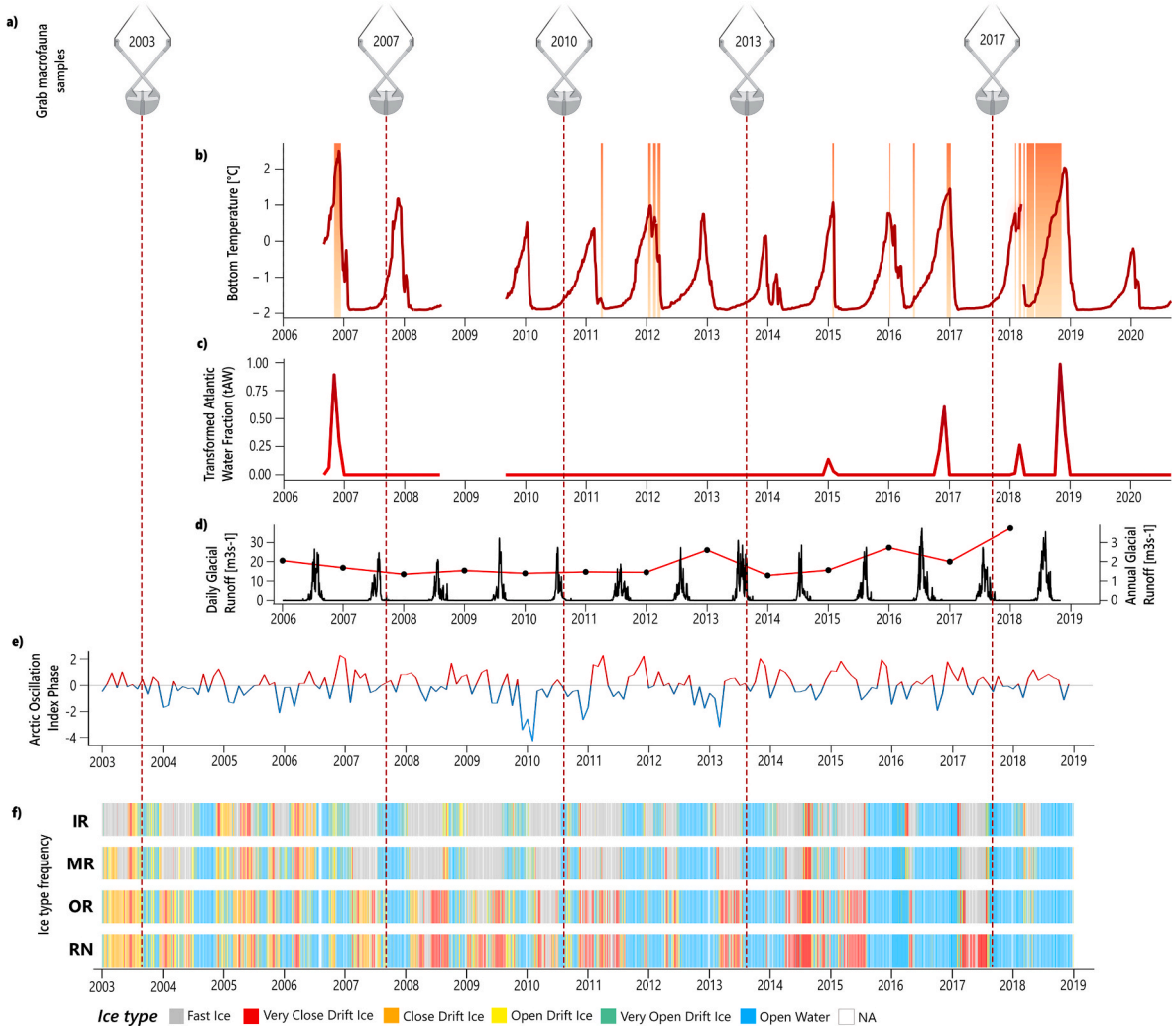

Fig. 2. Environmental variables throughout the study period. **a)** Times at which grab samples for the different years were taken are indicated with red dotted lines across all environmental variables **b)** Daily bottom water temperatures recorded at 200 m depth from the long-term mooring are indicated with a dark red continuous line (for location of mooring see maps Fig. 1). Gaps in the red line indicate non-available data. Periods shaded with orange indicate MHW events where temperatures are above the 90th percentile of the climatology baseline (based on 14 years of data) for more than five consecutive days. **c)** Transformed Atlantic Water (tAW) fraction (as the monthly average) at 200 m depth from the mooring defined as Temperature > 1 °C and Salinity >34.65 and represented by a red continuous line (gaps represent non-available data). **d)** Averaged daily glacial runoff (m^3/s) from four locations outside the discharge area of Rijpbreen (see Fig. 1c for location) based on runoff simulations from 2006 to 2019 (left axis with black line) and annual glacial runoff (m^3/s) from averaged daily runoff (right axis with red line and black dots) (Data courtesy of Jack Kohler, Norwegian Polar Institute (NPI)). **e)** Monthly Arctic Oscillation Index (AO) values from 2003 to 2018. Red lines indicate the positive phase of the AO, while blue lines indicate the negative phase. **f)** Sea-ice type frequencies for the four stations in Rijpfjorden (IR, MR, OR and RN) from 2003 to 2019. Each color band indicates a sea ice type based on the Norwegian Meteorological Institute (Ice Service) classification of ice types. Empty bands in white indicate no available data.

index ($H'_{(\log e)}$) and Pielou's evenness (J')) were calculated for each replicate sample with the "vegan" R package (Oksanen et al., 2020). To test for significant trends in total abundance, S, H', and J' over time and across stations, we built *generalized additive models* (GAM) with the "mgcv" package in R (Wood, 2011) for each of these response variables. The sampling years for each station were introduced as the smoothing parameter in the model ($k = 5$) together with the factor station as the predictor variables. For abundance and species richness, negative binomial family distribution was chosen with *log* as link function, whereas for H' and J' gaussian family distribution with *identity* link function was selected. Deviation, normality and homoscedasticity of residuals, together with the goodness of fit of observed values against response values were visually inspected with the function "gam.check" to identify violation of assumptions of the models (See Fig. A.2 to A.5).

2.4.2. Ordination and cluster analysis

In order to explore grouping patterns in species composition across time and space, non-metric multidimensional scaling (nMDS) analysis was performed with Euclidean distances derived from Hellinger transformed macrofauna abundance and presence-absence dissimilarities with the package "vegan". The Hellinger transformation was chosen to make the data suitable for Euclidean-based methods and to give a low weight to rare species (Legendre and Gallagher, 2001).

A cluster analysis using the UPGMA method was conducted with the R package "clustsig" (Whitaker and Christman, 2014) for the Hellinger transformed abundance data to support the patterns identified by the nMDS. Both nMDS and clustering were carried out with the averaged abundances and species occurrences for the three replicates at each station/year.

2.4.3. Beta diversity

The variation in community composition among sites in a region can be evaluated by calculating beta-diversity values (Whittaker, 1972). Changes in beta diversity can also be assessed through time and in the combination of time and space simultaneously (Legendre and Gauthier, 2014; Legendre, 2019).

Hellinger transformation was applied both to the abundance and occurrence data (each averaged over all replicates per station and sampling year) to calculate the beta diversity index (β_{TOTAL}) and the local contribution to beta diversity (LCBD) with the function "beta.div" of "adespatial" package (Dray et al., 2021) using Hellinger dissimilarity coefficients (Legendre and de Cáceres, 2013; Legendre and Borcard, 2018) between all stations and years. LCBD indices represent the degree of uniqueness of the samples in terms of community composition (Legendre and de Cáceres, 2013) and show how much each observation contributes to beta diversity; a sample unit with an LCBD value of 0 would have the species composition of the average centroid for all sites. LCBD values can be tested for statistical significance by random, independent permutations of the species matrix. Adjusted p-values (Holm correction method for multiple testing) for the LCBD values were calculated with 999 permutations, testing the null hypothesis (H_o) that species are randomly distributed and independent of one another across the sites/time (Legendre and de Cáceres, 2013).

When assessing diversity fluctuations in biological communities, it is of interest to disentangle the potential underlying ecological mechanisms by which species compositions change through time and space, i.e. how they disassemble and reassemble (temporal turnover) (Tatsumi et al., 2020). The change in beta diversity ($\Delta\beta_{TOTAL}$) among two or more sites throughout two time points can be either caused by *disappearances* (extirpations, $\Delta\beta_E$) or by *increases* (colonizations, $\Delta\beta_C$) of species (Olden and Poff, 2003; Tatsumi et al., 2021). Both extirpations and colonizations can lead to homogenization ($\Delta\beta_{E-}$ and $\Delta\beta_{C-}$) of species composition among the sites, i.e., decreasing β_{TOTAL} ($-\Delta\beta_{TOTAL}$), or to heterogenization ($\Delta\beta_{E+}$ and $\Delta\beta_{C+}$) of species composition between sites, i.e., increasing β_{TOTAL} ($+\Delta\beta_{TOTAL}$) (Tatsumi et al., 2021). $\Delta\beta_E$ and $\Delta\beta_C$ can be further decomposed into two more components (Type 1 or 2) depending on whether the colonization or extirpation of the species in question appear ($\Delta\beta_{C-}$ Type1) or disappear ($\Delta\beta_{E-}$ Type 1) at both sites simultaneously or at just one site ($\Delta\beta_{C-}$ Type2, if incoming species at one site were already initially present at the other; and $\Delta\beta_{E+}$ Type 2, when species disappearing at one site were initially present at both sites) (See Fig. A.1 for a visual description of the colonization-extirpation processes and how they affect the change in beta diversity among sites, adapted and modified after Tatsumi et al. (2021)). The relative contribution of each component can indicate different ecological processes. For instance, contributions of $\Delta\beta_{E-}$ might reflect stochastic extirpations of regionally rare species, while a greater contribution of $\Delta\beta_{E+}$ might be a sign that widespread species are decreasing more in frequency than rare species (Tatsumi et al., 2021). High $\Delta\beta_{C-}$ could reflect the appearance of species with high dispersal capacity, spreading across all sites, or internal dispersion of species to new sites that were once restricted by a dispersal barrier. Finally, $\Delta\beta_{C+}$ can occur when new species are added to unique locations. All four components of contribution to $\Delta\beta_{TOTAL}$ can happen simultaneously, potentially cancelling each other out, which is the reason why decomposing these changes can help to recognize the underlying fluctuations in species composition that are taking place. Beta diversity values (β_{TOTAL}) using the Sørensen index were calculated between IR and OR for each year for the presence-absence transformed macrofauna data. Following that, we calculated $\Delta\beta_{TOTAL}$ and its decomposition into its components of $\Delta\beta_C$ and $\Delta\beta_E$ (and their respective homogenization and heterogenization components: $\Delta\beta_{E-}$, $\Delta\beta_{C-}$, $\Delta\beta_{E+}$ and $\Delta\beta_{C+}$) for each time period using the "ecopart.pair" function within the "ecopart" R package (Tatsumi, 2022).

To test whether station IR or station OR changed more exceptionally with respect to one or the other in time, and to evaluate if the sill could have played an important role dampening effects of community change at the inner station, the temporal beta diversity index (TBI) was calculated (Legendre, 2019) using the percentage difference index (%diff) for both abundance and occurrence data with the "TBI" function of the R package "adespatial". TBI indices measure the change in community composition between two time points (T1 and T2) (Legendre, 2019), generating a vector of TBI dissimilarities for each site. A random permutation test (999 permutations) was used to test for significance of the TBI indices and p-values were corrected for multiple testing using the Holm method (Legendre, 2019). Furthermore, the TBI dissimilarities between the two time points at each site were decomposed into contributions from losses (B) and gains (C) of species and abundances (Legendre, 2019).

2.4.4. Variation partitioning of temporal and environmental drivers on macrofauna composition

Redundancy analysis (RDA) was used to partition the variation within the macrofaunal data on a set of environmental predictor variables and a second set of temporal predictor variables (see below), for each station individually (Borcard et al., 1992).

All environmental variables (see section 2.4) were included in the set of environmental predictor variables. The sum of frequencies for each type of ice was calculated for each station over the period of one year prior to each sampling event for macrofauna (to account for time lags of possible integrated sea ice cover effects on macrofauna communities) and were used as environmental variables for constrained ordination analysis. Only stations IR, OR and RN for the period between 2007 and 2017 were used for the analysis (due to missing ice data for year 2002). When using the sea ice frequency as a constraining variable for the macrofauna variation, we grouped the frequencies of the categories for open water and very open drift ice under the category of "open water", and very close drift ice, close drift ice and open drift ice in the category "drift ice".

Asymmetric Eigenvector Maps (AEMs) were used as temporal predictor variables (Legendre and Gauthier, 2014). AEM is an eigenfunction method suitable to model multivariate directional processes like temporal change of species abundance data. By incorporating AEMs as constraining temporal predictors one can account for temporal autocorrelation (or temporal structure) in the abiotic drivers or in the species matrix itself (Legendre and Gauthier, 2014). AEMs were calculated for the sampling period with complete environmental data sets available (i.e. 2007 – 2017). To account for the irregular intervals between sampling events, dummy sampling events were added in mid-August (15th August) for years when no samples were collected. AEMs were then calculated using the time between neighboring dates as edge weight with the function "aem.time" from R package "adespatial". In principle, AEMs of time essentially produce n-1 sine waves of decreasing wavelength (n = total number of sampling dates; here n = 11 due to dummy variables). Accordingly, the first AEM (AEM_1) describes a one directional change throughout the entire study period, while the last AEM (AEM_{10}) describes alternating changes from year to year (fine temporal scales).

Prior to variation partitioning, both sets of predictor variables were individually subjected to forward selection using a double-stopping criterion (Blanchet et al., 2008) to avoid overestimation of the explained variation. In this approach, variables are added to the model in order of decreasing explanatory power until no variable adds significantly to the explanatory power or until the $R^2_{adjusted}$ exceeds the $R^2_{adjusted}$ of the full model. The variation partition analysis was performed with the "varpart" function of the R package "vegan".

3. Results

3.1. Environmental variables

The highest bottom water temperatures at 200m depth, reaching above 2 °C, were recorded by the end of 2007, coinciding with the first

SfWWTA recorded in Rijpfjorden (Fig. 2b) which lasted for 40 days. A succession of three shorter SfWWTAs (of between 16 and 18 days each) were recorded at the beginning of 2012. Following that, another SfWWTA (of 25 days) with the second highest temperature values since 2006 occurred by the end of 2016. SfWWTAs were recorded for most part of the year in 2018 (Fig. 2b).

At all stations inside the fjord, the averaged bottom water temperatures from all years of the CTD casts was <0 °C, emphasizing the overriding influence of Arctic characteristics in this system, with winter cold bottom water (WCW), while the outer station RN had average temperatures above 0 °C with the highest temperature recorded of 2.75 °C (Table 1). Bottom water salinity values across all stations and years ranged from 34.6 to 34.9.

The monthly Arctic Oscillation Index (AO) (Fig. 2e) showed the most negative values in early 2010 and early 2013. The highest peaks of positive AO values were observed at the end of 2006 and at the beginning and end of 2011. No clear trends were observed, but between 2009 and 2010 the AO index was more negative than other periods of time.

The daily average glacial runoff for the four locations around the Rijpbreen discharge area was seasonal, with high runoff in the summer months. Peak flows were the highest for 2009, 2013 and 2016 (Fig. 2d). Annual average of daily runoff values ranged between 1.29 m^3/s in 2014 and 2.74 m^3/s in 2016 over the study period. Although year 2018 was not included in the macrofauna time series, annual runoff values for that year were the highest of all with 3.75 m^3/s. Annual runoff values appeared to be more variable from 2012 onwards.

The innermost stations (IR and MR) were dominated by local fast ice, while the outer station (OR) and the shelf station (RN) had a higher frequency of drift ice (Fig. 2f). From 2012 onwards, prolonged periods of open water became more frequent at all stations.

3.2. Macrofauna community fluctuations in time across the fjord axis

3.2.1. Abundance and alpha-diversity

A total of 345 taxa belonging to 104 families and to 11 phyla were identified. The most abundant classes were Polychaeta (71%), followed by Bivalvia (21.6%).

Both abundance and species richness followed similar statistically significant trends across years for all stations with more than 2 sampling events (see Fig. 3 for significance of results and Table A.1 for detailed output of GAM models) (Fig. 3b and c), indicating big fluctuations through time. On average, abundance at IR and OR in 2007 was respectively between 0.2 and 0.8 times that in 2003, and for richness between 0.7 and 0.5 times. After these decreases, both variables followed a strong increase: on average, abundance at IR, OR and RN in 2007 was respectively between 5.4, 12.4 and 7.3 times that in 2003, and

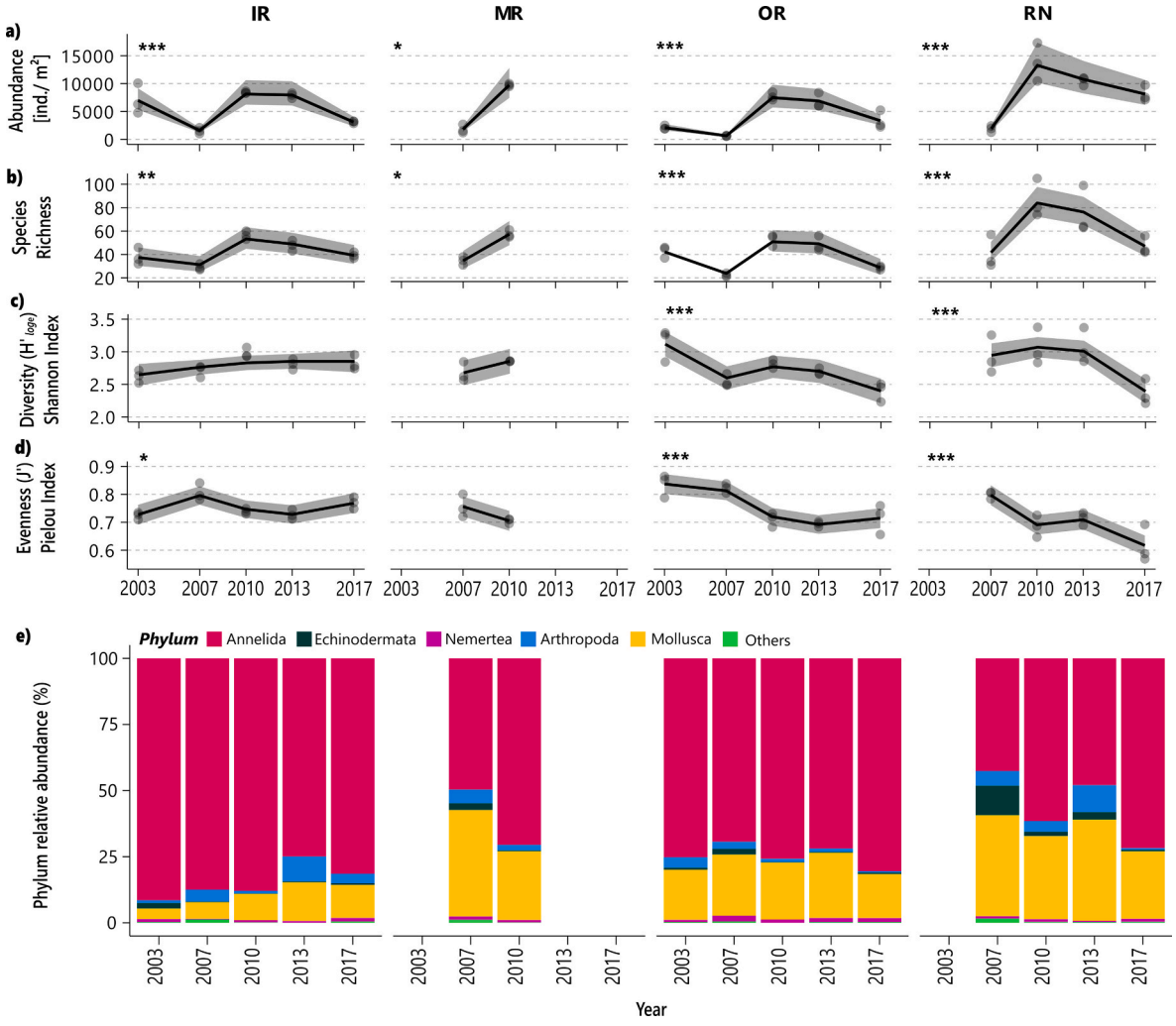

Fig. 3. Macrobenthic community metrics along the Rijpfjorden axis through time. **a)** abundance (ind./m^2), **b)** species richness, **c)** Shannon index (H′), **d)** Pielou's evenness index (J′). Significance of variation across years for each station from the GAM models is indicated with *** = p-value <0.001, ** = p-value 0.001–0.01, * = p-value 0.01–0.05 at the top of each panel. Shading represents the 95% confidence interval. **e)** Relative abundance by phylum for each station across time (averaged for three replicates). Empty data is missing data (no sampling of macrofauna).

for richness between 1.9, 2.3 and 2.1 times. After 2010, both variables decreased again.

H' showed significant changes through time at stations OR and RN (Fig. 3c), with a significant drop from 2003 to 2007 at OR. Hardly any change in H' from 2007 until 2013 was observed at both stations, followed by a significant decrease from 2013 to 2017 at OR. Highly significant decreases in J′ occurred at the outer stations (OR and RN), while significant (IR) or non-significant (MR) fluctuations were observed in the inner part of the fjord (Fig. 3d).

In all years, Annelida dominated relative abundances at the inner station (>75%) and at the outer station OR (c.a. 75%) (Fig. 3e). Mollusca were abundant in some years at station MR and RN. At RN, there was an increase in the relative contribution of Annelida to total abundances in the most recent years.

At station IR, most abundant families were Cirratulidae and Lumbrineridae, except for year 2007 (Fig. 4). At station MR, Thyasiridae dominated from 2010 onwards. At station OR, Cirratulidae and Thyasiridae families dominated after 2007, and for station RN, Oweniidae, Thyasiridae and Yoldiidae were the dominant families after that year as well.

3.2.2. Ordination and cluster analysis

The community structure of the inner station (IR) was clearly distinct from all other stations in the abundance-based nMDS (Fig. 5a), indicating a spatial differentiation. Additionally, a temporal pattern was observed for stations MR, OR, and RN. These stations grouped together from 2010 onwards, while samples from 2003 to 2007 were more distant from this group. In the occurrence-based nMDS (Fig. 5b), a dominant temporal structure was observed. Samples collected in 2003 and 2010 grouped together, while all samples from 2013 to 2017 were more similar to each other than to other years. Samples from 2007 appeared to group farther apart (with the exception of station IR which grouped

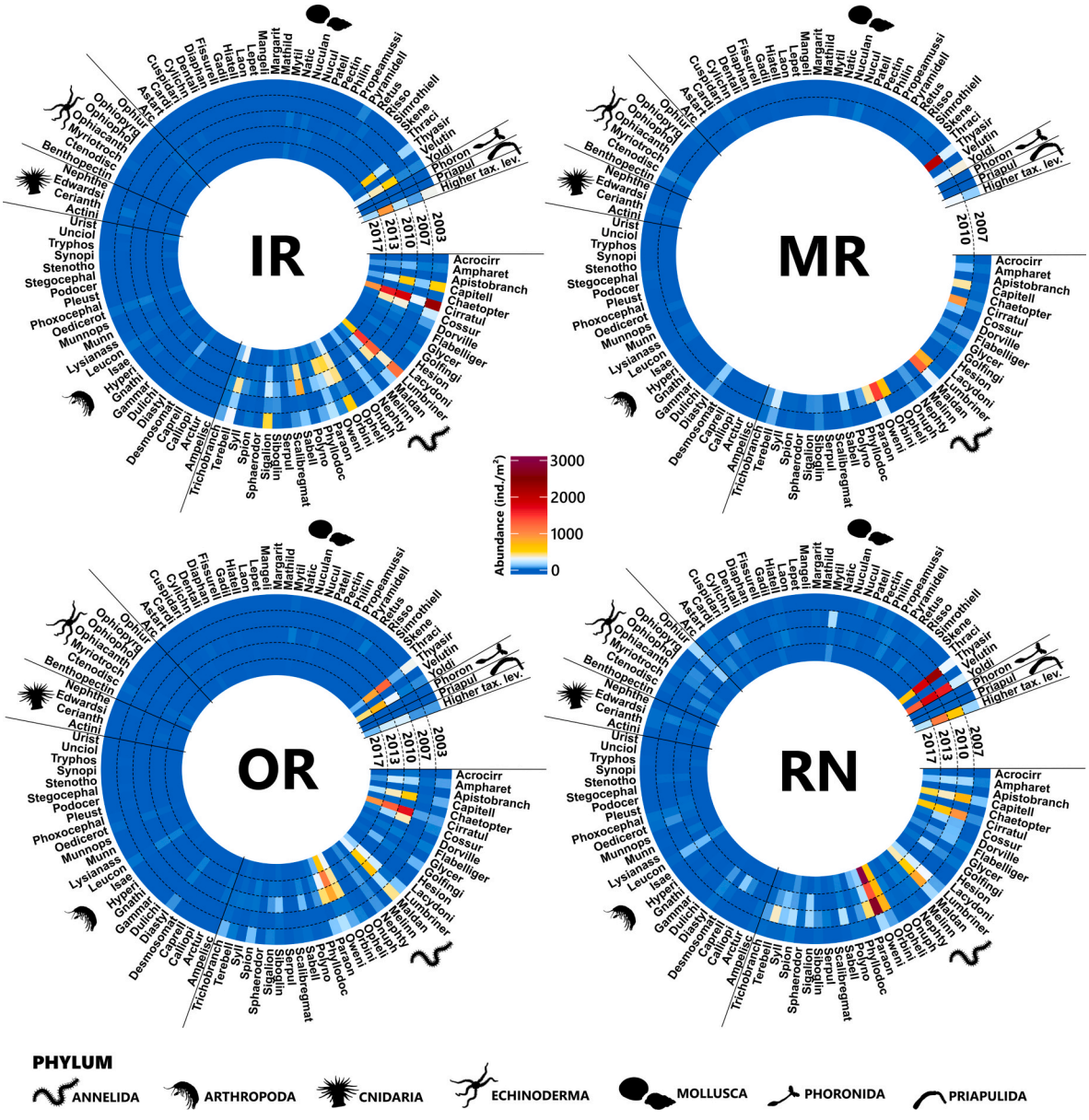

Fig. 4. Heatmaps showing averaged abundances (three replicates) for each Family (note that suffix -idae is missing at the end of each family name for space reasons). Each circle represents one station (IR, MR, OR and RN) and each concentric line represents the different years (2003, 2007, 2010, 2013 and 2017). Families are grouped by phylum (indicated by pictograms at the bottom). The last category belongs to taxa only identified to higher taxonomic level than family. Abundances are given as individuals/m^2 with dark blue representing lowest values and dark red/fuchsia representing highest values (see color scale in the middle). Phylum pictograms modified after Integration and Application Network (IAN) library symbols and PhyloPic.

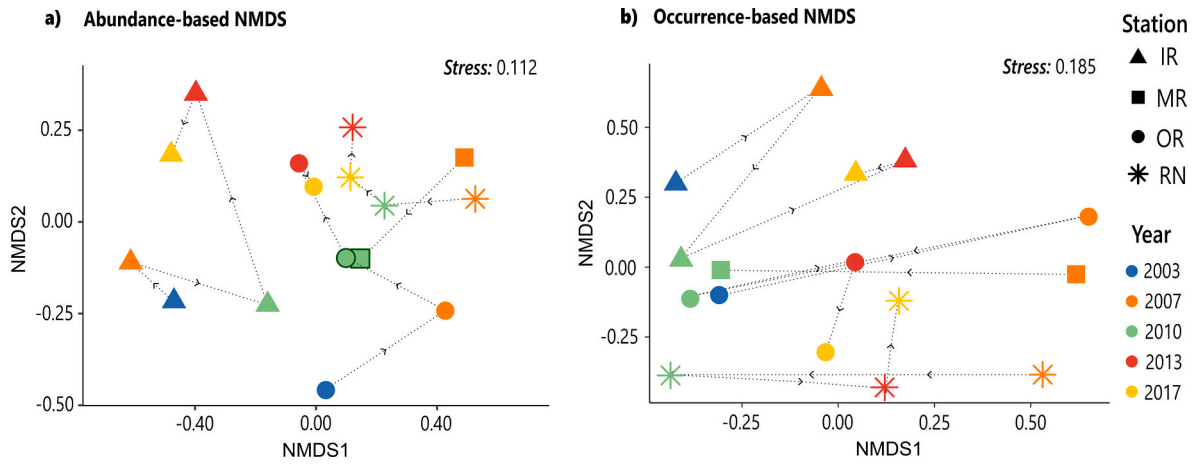

Fig. 5. Two-dimensional nMDS plot of: **a)** Hellinger transformed macrofauna abundance and **b)** Hellinger transformed occurrence data. Colors indicate the year of macrofauna sampling while symbols indicate the four different stations (for station codes and geographical location see Fig. 1). Black dotted lines with arrows track the direction of change at each station from year to year in the ordination space.

closer to the ones from 2013 to 2017).

The UPGMA cluster confirmed the nMDS patterns for the abundance-based dataset (Fig. 6). The most abundant taxa for the IR samples were lumbrinerid (*Lumbrineris mixochaeta, Scoletoma* sp.) and cirratulid polychaetes (*Tharyx* sp., *Aphelochaeta* sp.). Dominant taxa at stations MR, OR and RN included several different polychaetes (*Galathowenia oculata*, *Chaetozone* sp., *Maldane* spp.) and bivalves (*Mendicula* sp., *Yoldiella* spp. – Fig. 6) from 2010 onwards. Other polychaete species such as *Maldane* spp., *Heteromastus filiformis,* and *Leitoscoloplos mammosus* were also abundant at those stations after 2010, but less than the others.

3.2.3. *Beta-diversity*

The spatio-temporal LCBD values obtained from the abundance-based macrofauna data (Fig. 7a) indicated higher values for all samples from 2003 to 2007, together with most samples in all years at the IR station, indicating a more distinctive species composition at IR than at stations MR, OR and RN and from 2010 onwards (with lower LCBDs). However, no significant differences were detected after the permutation test for any of the station/year. In contrast, for the presence-absence dataset, the LCBD map showed lower values for years 2003 and 2010 than for 2013 and 2017 (Fig. 7b). All samples from 2007 presented the highest values, but only samples from OR and RN stations showed statistically significant uniqueness in species composition after the permutation test.

Beta diversity values between stations IR and OR (Fig. 8a), based on the presence-absence data, showed an increase between 2003 and 2007, and then a large decrease between 2007 and 2010, with the lowest values for 2010. From then onwards, beta diversity increased again gradually.

Temporal changes in beta diversity between IR and OR were mainly driven by colonization. Extirpations of species, in contrast, appeared not to contribute much to beta diversity changes through time ($\Delta\beta_E$ values were close to 0) (Fig. 8b). Nonetheless, when further decomposing its components into attributes of homogenization and heterogenization (Fig. 8c), we found that extirpation contributions had in fact higher values than those of colonization. However, extirpations (both $\Delta\beta_{E-}$ and $\Delta\beta_{E+}$) almost canceled each other out at all time periods. When further decomposing $\Delta\beta_{E+}$ into type 1 and 2, both types equally contributed to $\Delta\beta_{TOTAL}$ during all periods except for 2013–2017, when $\Delta\beta_{E+}$ was dominated by contributions of type 2 (Fig. 8d). Between 2007 and 2010, colonization ($\Delta\beta_C$) of taxa dominated the $\Delta\beta_{TOTAL}$ over extirpations ($\Delta\beta_E$), especially driven by contributions of $\Delta\beta_{C-}$, indicating establishment of widespread species common at both stations. This contribution by $\Delta\beta_{C-}$ was mainly dominated by type 1 colonization, while for the last period 2013–2017 was dominated by type 2 colonization (Fig. 8d). In order to be able to interpret the results from all different components of contributions to change in beta diversity we looked at the number of taxa appearing and disappearing exclusively at each station (IR and OR) and at both stations simultaneously for each consecutive time period (Fig. A.6).

The average dissimilarity at each site (IR and OR) between each period showed a similar pattern for both abundance and occurrence-based data (Fig. 9). On average, the communities at both sites changed more during the first two periods (2003–2007 and 2007–2010), while lower dissimilarities were observed from 2010 onwards. Between 2003-2007 and 2013–2017, changes were on average dominated by losses in species (or abundance), while for 2007–2010 gains dominated at both sites. TBI permutation tests showed that station OR changed more significantly in species composition than IR between 2003 and 2007 for the occurrence dataset. While no significance was reported after p-value correction, station IR changed more than OR between 2010-2013 and 2013–2017 for the abundance-based dataset (with p-values close to significance of 0.06) (Fig. 9 and Table A.2).

3.3. *Variation partitioning of environmental and temporal drivers*

For station IR, selected environmental drivers of macrofauna community variation were glacial runoff and AO index; for station OR, bottom temperature and glacial runoff; and for RN, bottom temperature, open water frequency and bottom salinity (Fig. 10).

All temporal AEMs generated from the distances between sampling events were also subjected to forward selection at each station. The order of the selected AEMs increased from the shelf station RN (AEMs 5, 3 & 4), toward the outer fjord (OR: AEMs 5 & 9) and further towards the inner basin (IR: AEMs 6 & 9 (Fig. 10).

At station IR, the variation partitioning indicated that throughout 2007, 2010, 2013 and 2017 the selected environmental variables accounted for 12% of the variation in the macrofauna. At the same time, 13% of the variation was also accounted for by the selected temporal predictors, and a total of 27% was explained by the temporal structure of the environmental variables. For station OR, the selected environmental variables only explained 4% of the macrofauna variance, 7% was explained by the temporal AEMs but 38% in combination with the temporal predictors selected. Lastly, for the outer-most station, RN, the environmental variables selected only explained variation in the macrofauna when combined with the selected temporal AEMs (up to 30%).

4. Discussion

Our time series shows that macrofaunal composition fluctuations

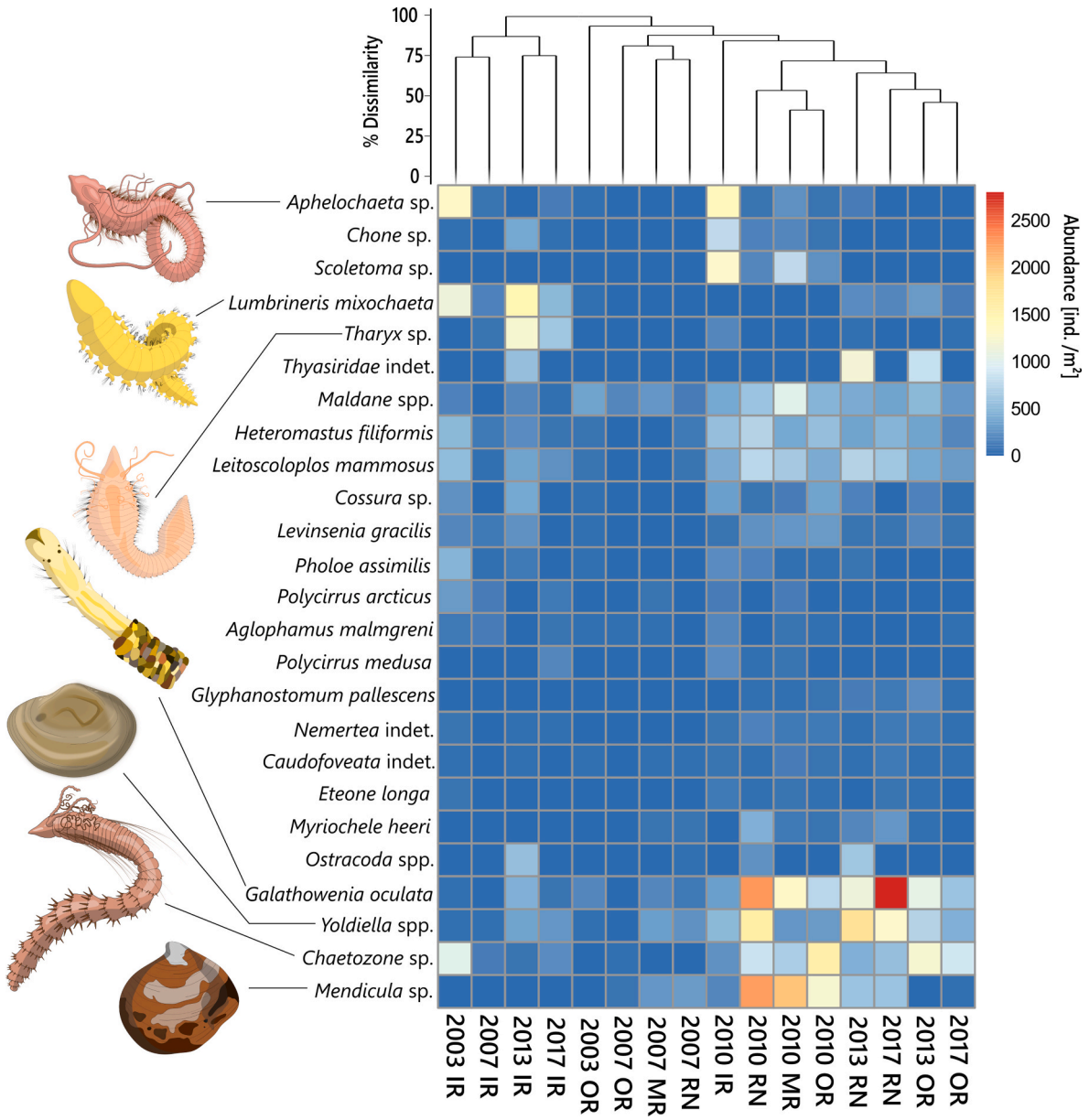

Fig. 6. Cluster derived with the UPGMA method based on Hellinger transformed macrofauna abundances (ind. m^{-2}) of the whole macrofauna community, averaged for the three replicates. The heatmap shows only taxa with more than 500 ind. m^{-2} throughout the whole time series. Color scale indicates raw abundance values (ind./m^2). Drawings for some of the most abundant species are presented (Drawn by: Èric Jordà Molina).

took place in Rijpfjorden during the first two decades of the 21st century, and occurred in conjunction with longer open water periods and times of documented seafloor warm water temperature anomalies (SfWWTAs). We identified three distinct periods of change: a strong disturbance, subsequent recovery, and then a gradual restructuring of macrobenthic communities. We also confirmed that the outer stations were more prone to significant changes in macrofauna species composition through time than the inner silled basin, although this last one also experienced fluctuations.

4.1. 2003–2007: a strong Atlantic inflow in 2006 led to macrofauna extirpations across Rijpfjorden, with less impact in the inner-basin

The mooring at station MR recorded SfWWTAs of up to +2 °C between August and November 2006 (Fig. 2b). Temperature anomalies were also documented in many other western fjords of the archipelago for that year (Bloshkina et al., 2021). At the same time, a significant increase in surface water temperature defined as a warm water anomaly was observed between 2004 and 2008 at the Fram Strait region (Beszczynska-Möller et al., 2012), which translated rapidly into changes in several marine biological components (Soltwedel et al., 2016), from zooplankton communities (Ramondenc et al., 2002) to the seafloor. For instance, studies from the Long-Term Ecological Research HAUSGARTEN observatory, in the deep Fram Strait, revealed that nematode densities between 2000 and 2009 suffered a drop from 2002 to 2005, and bounced back after 2006 (Hoste et al., 2007; Grzelak, 2015; Soltwedel et al., 2016). Our results suggest that this warm water anomaly, reflected as a potential benthic MHW in our mooring data, reached to northern Svalbard fjords and had significant impacts in the macrofauna communities from Rijpfjorden, also reflected as drops in abundance and species richness in 2007 (Fig. 3a and b). The changes in community composition translated into an increase in beta diversity between the inner and outer stations (IR and OR) (Fig. 8a), and although this change was mainly caused by colonizations at one site, further decomposition

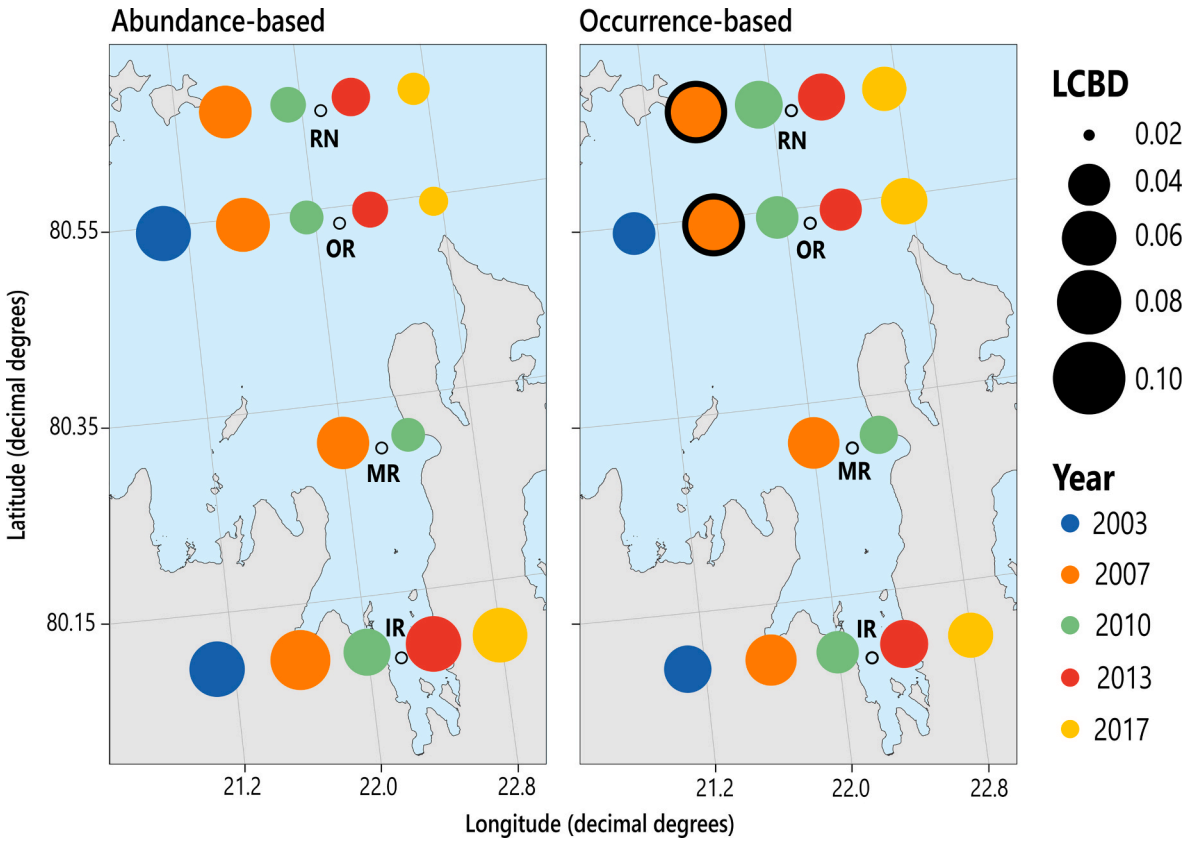

Fig. 7. Local contributions to beta diversity (LCBD) map over time and space for abundance based (left) and occurrence based (right) macrofauna datasets. The size of the bubbles is proportional to the LCBD values and the different colors indicate the year of macrofauna sampling. Black rims around the bubbles indicate LCBD p-values that are significant in the permutation test after the Holm correction (alpha = 0.05).

revealed that important widespread and local extirpations took place (Fig. 8b and c). Mass mortality events (MMEs) among benthic communities have been reported in other marine ecosystems after MHWs. For example, in the Mediterranean Sea, decreases in especially sessile organisms were observed and correlated with the temperature anomalies recorded for the summer of 2003 (Garrabou et al., 2009), while throughout the last decades, five consecutive MMEs associated with more recent MHWs have taken place (Garrabou et al., 2022).

We found supporting evidence for our hypothesis that the macrobenthos of the inner-most silled basin would remain more stable due to dampened fluctuations in environmental conditions compared to the outer sties. Both the nMDS (Fig. 5) and the LCBD indices partially supported this hypothesis, since the magnitude of change at station IR after the SfWWTA of 2006 (2003 vs 2007 years) was smaller than for the outer stations, and LCBD indices were only significant for the outer stations in 2007 (Fig. 7). Both alpha (H′) and beta diversity analyses also supported the possibility of partial protection by the sill. For instance, from the TBI analysis we saw that station OR changed significantly in beta diversity for this period compared to station IR (Fig. 9), and H' plummeted significantly at OR while it remained stable at IR (Fig. 3c). The distinction of macrobenthic communities between inner and outer parts of silled fjords seems to be a common feature in Arctic and sub-Arctic silled fjords (Włodarska-Kowalczuk et al., 2005; Renaud et al., 2007; Kędra et al., 2010; Jordà-Molina et al., 2019; Udalov et al., 2021). The shallow sill of Rijpfjorden, therefore, seems to protect the inner basin from macrofauna fluctuations to certain extent, but not completely as indicated by the widespread non-random extirpation contributions of taxa occurring across the fjord axis during this period, including the inner parts of the fjord, and also indicated by significant drops in abundances at this inner location (Fig. 8c, Fig. A.8).

4.2. 2007–2010: a recovery period with widespread re-colonization resulting in homogeneous fjord macrobenthos

Our results indicate that the period 2007–2010 was a recovery phase for the macrobenthic communities after the disturbance event of 2006. During this period with prevailing cold water temperatures and longer-lasting sea-ice cover, change in total beta diversity between IR and OR was dominated by contributions of colonizations leading to a decrease in beta diversity, which was mainly driven by widespread species arriving at both sites (from other areas of the fjord not covered in the sampling or from outside the system) (Fig. 8a,b,c). Such a widespread colonization from outside the fjord led to homogenization of benthic communities. Such evidence of homogenization in macrofauna assemblages of previously distinct fjordic regions (mainly in outer and mid-fjord areas) has also been observed in Kongsfjorden (Kędra et al., 2010), which the authors attributed to the increased inflow of AW into the fjord due to a more enhanced West Spitsbergen Current (WSC) transport during the first decade of the 21st century.

The significant increases in abundance and species richness, and moderate increases in H′ reported in most sites across Rijpfjorden between 2007 and 2010 support this recovery scenario through re-colonization (Fig. 3a,b,c). Furthermore, the significant drops in J' for the outer stations indicate that a few taxa already present before the extinction event started dominating the community after 2007 (Fig. 3d). These taxa include *Galathowenia oculata*, *Yoldiella* spp., *Chaetozone* sp., and *Mendicula* sp., followed in lower abundance by *Maldane* spp., *Heteromastus filiformis,* and *Leitoscoloplos mammosus* (Fig. 6). All these species also appeared in the inner station but at much lower abundances. Most of these taxa are opportunists with ranges spanning well into boreal/temperate regions, and capable of strong fluctuations in population size over short periods of time. For example, *G. oculata,* which had

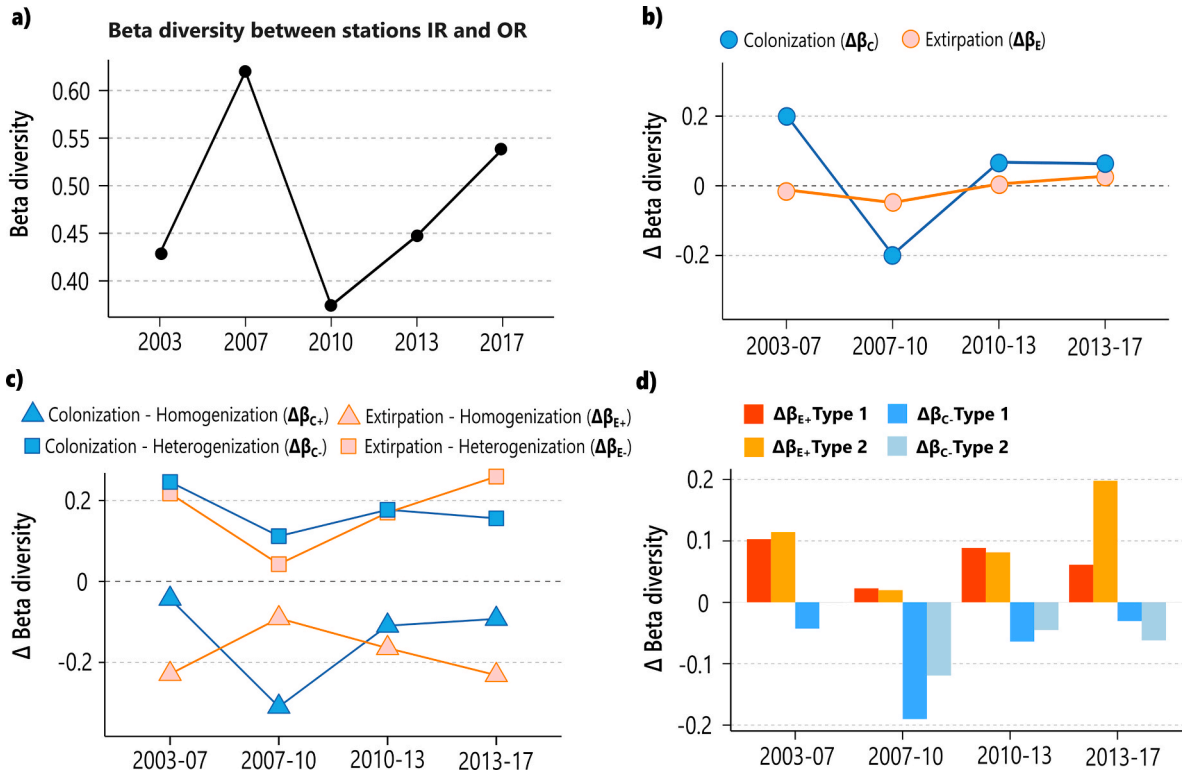

Fig. 8. Changes in beta diversity between stations IR and OR over time. **a)** Sørensen beta diversity values between stations IR and OR for each year for the occurrence macrofauna community data. **b)** Decomposition of temporal change in beta diversity into contributions by colonization ($\Delta\beta_C$) and extirpation ($\Delta\beta_E$) for each consecutive period. **c)** Decomposition of temporal change in beta diversity into contributions by colonization resulting in heterogenization ($\Delta\beta_{C+}$) (blue squares) and homogenization ($\Delta\beta_{C-}$) (blue triangles) and by extirpations leading to heterogenization ($\Delta\beta_{E+}$) (red squares) and homogenization ($\Delta\beta_{E-}$) (red triangles). **d)** Decomposition of $\Delta\beta_{E+}$ into Type 1 (red) and Type 2 (orange) and $\Delta\beta_{C-}$ into Type 1 (dark blue) and Type 2 (light blue). For interpretation of the $\Delta\beta_{E+\ Type\ 1}/\Delta\beta_{E+\ Type\ 2}$ and $\Delta\beta_{C-\ Type\ 1}/\Delta\beta_{C-\ Type\ 2}$ the reader is referred to Fig. A.1 of Appendix.

the highest abundances recorded in the time series, is a surface-deposit feeding tube-building polychaete that has been described as tolerant to environmental stressors such as sedimentation loads or organic enrichment and seems to be facilitated by slight disturbances (Trannum et al., 2022). Although we do not have sediment parameters for all years, TOC values for 2003–2010 (Table 1) for the top 2 cm of the sediment indicate a slight increase in organic carbon content for stations IR and OR (from 1.19 to 1.35% and from 1.44 to 1.66% respectively). This potential increase in food availability, although highly speculative, and the ecological space made available after the massive extinctions seen in 2006 could have contributed to the success of disturbance-tolerant taxa such as *G. oculata, H. filiformis,* and *Chaetozone* sp. Studies comparing macrobenthic samples of the Fram Strait from the year 2000 (before the warm water anomaly recorded in that region) vs. 2010 and 2017 (after the warm water anomaly), revealed significant shifts in macrofauna community composition, with generalized increases in density and diversity across all depths from shelf to basin following a transect at 79°N starting at the shelf off West Spitsbergen (outside of Kongsfjorden) for the latter (Górska et al., 2022). In this case, some of the taxa that experienced highest increases in 2010 at the shelf stations (70–400 m depth) were some of the same representatives that we saw increasing in Rijpfjorden. This was accompanied by increases in food availability (e.g. sediment-bound chloroplastic pigments) at the seafloor from 2007 onwards (Soltwedel et al., 2016). This could indicate that the shift in productivity and food availability at the seafloor recorded in the Fram Strait, could have been observed as well in the northern fjords from Svalbard.

4.3. 2010–2017: the inner and outer areas slowly re-assemble and diverge in structure

For the last two survey periods (2010–2013 and 2013–2017), beta diversity increased gradually between IR and OR (Fig. 8a). We found indications that widespread species that were initially shared at both IR and OR in 2010 disappeared during 2010–2013, contributing to heterogenization between IR and OR. (Fig. A8). However, contributions to change in beta diversity from both widespread and local extirpations cancelled each other out, making contributions of colonizations leading to heterogenization the ones driving the overall beta diversity change. This establishment of new taxa exclusive to each site (especially at station IR (Fig. A8) increased the $\Delta\beta_{TOTAL}$ for this period (Fig. 8a). Although SfWWTAs were detected in early 2012, no tAW was associated with them (Fig. 2b and c). Perhaps this indicates that water from the shelf was advected into the fjord but was heavily mixed with local water, maintaining a higher temperature than the receiving water at that time of the year (late winter). Whether this advective event had any impacts on the recruitment or settlement of benthic larvae is something worth considering, but it seems that this SfWWTA during winter time did not have such a drastic impact as in 2006 on the macrobenthic communities. Interestingly, between 2013 and 2017, the extirpation contributions to $\Delta\beta_{TOTAL}$ (both $\Delta\beta_{E+}$ and $\Delta\beta_{E-}$) (Fig. 8c) had higher values than both components of contributions due to colonization, and most of the heterogenization caused by extirpations was due to the disappearance of species previously common at both sites which disappeared from one of them ($\Delta\beta_{E+}$ Type 2). In fact, although extinctions of taxa exclusive to each site were almost equal (26 and 28 taxa for IR and OR respectively), extirpations at OR from taxa initially shared with IR accounted for 11 taxa, while 6 shared taxa went lost at station IR (Fig. A8). This indicates that the two stations had begun to re-assemble in a divergent manner. It

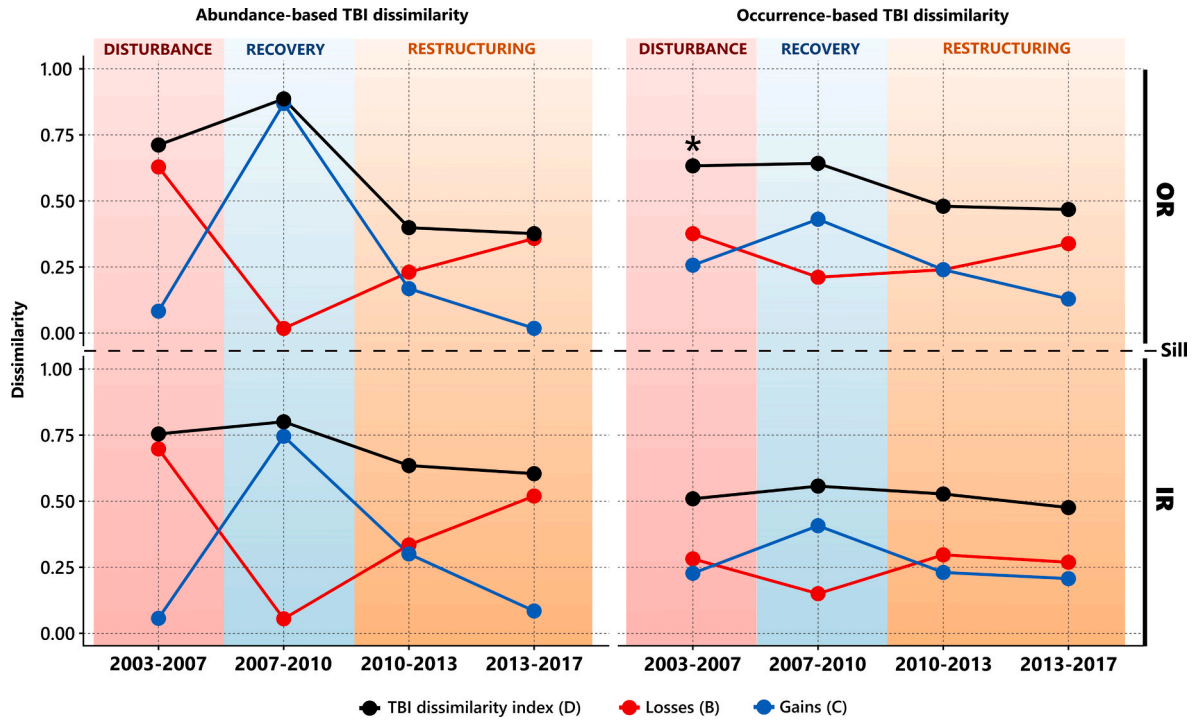

Fig. 9. Temporal beta diversity indices (TBI), calculated with *%diff* dissimilarity index, for the abundance-based (left) and occurrence-based (right) macrofauna and for each station: outer Rijpfjorden (OR, top) and inner Rijpfjorden (IR, bottom) which are physically separated by a sill. The dissimilarity in community composition (abundance or occurrence-based) between years of consecutive intervals at each station is depicted with black dots and lines (that is the total dissimilarity in time (D) which is equivalent to the TBI index). The TBI dissimilarity (D) is then decomposed in abundance or taxa losses (B) represented by red dots and lines, and gains (C) indicated with blue dots and lines. The sum of (B) and (C) is equal to (D). The asterisk (*) at station OR for the period 2003–2007 indicates that this station changed significantly compared to station IR for that time interval (based on the TBI permutation test, with 999 permutations, alpha = 0.05, p-value = 0.04 after Holm correction).

is also possible that the inner station started acting as a refugium for some species present in the outer parts of the fjord during the last AW intrusion, as fewer shared taxa were lost at IR than at OR.

4.4. Spatio-temporal drivers of change in macrofauna communities

The macrofauna communities of the outer stations of Rijpfjorden changed following long temporal patterns, as they were linked with long-term hydrographic trends that we have documented in this fjord potentially reflecting the SfWWTAs. However, the innermost locations followed more stochastic shifts (as indicated by the higher selected AEMs), pointing towards more complex environmental interactions and temporal changes towards the head of the fjord (Fig. 10).

In high Arctic fjords, it is well understood that glacial runoff from adjacent glaciers plays a key role in structuring seafloor communities (Holte and Gulliksen, 1998; Udalov et al., 2021; Włodarska-Kowalczuk et al., 2005; Włodarska-Kowalczuk and Pearson, 2004). This is mainly due to high sedimentation rates of inorganic material that increase towards high glacial activity areas (usually in glacial bays at the head of fjords) diluting food particles at the seafloor and promoting the burial of fauna. Hence, suspension feeders and filter feeders are usually negatively affected by these sedimentary loads, clogging their feeding organs, while relatively motile surface and sub-surface deposit feeders, carnivorous/omnivorous, and predators thrive better in these unstable and stressful conditions (Włodarska-Kowalczuk et al., 1998). This was reflected in the community of the inner-most station of Rijpfjorden, which was dominated by the carnivorous polychaetes *Lumbrineris mixochaeta* and *Scoletoma* sp. as well as surface deposit feeders like the cirratulid polychaetes *Aphelochaeta* sp., *Chaetozone* sp. and *Tharyx* sp. (Fig. 5). Some of these taxa have also been found to be common in inner parts of other silled fjords of Svalbard (i.e. Kongsfjord and van Mijenfjord; (Włodarska-Kowalczuk and Pearson, 2004; Renaud et al., 2007; Kędra et al., 2010). Sedimentation-tolerant nuculanid and thyasirid bivalves have also been reported as co-dominant taxa in inner glacial sites in other Arctic fjords (Udalov et al., 2021), but were only found in low densities in inner Rijpfjorden. Vertical fluxes of organic and inorganic material have been reported to be an order of magnitude higher in Kongsfjorden than in Rijpfjorden (Weydmann-Zwolicka et al., 2021). The relatively low sedimentation in Rijpfjorden might cause carnivore polychaetes to thrive better than the partially infaunal deposit-feeding bivalves (McMahon et al., 2006), perhaps outcompeting the latter. Therefore, it appears to be important to consider the degree of sedimentation impact in high Arctic fjords, as it could give place to unique inner-communities as seen in Rijpfjorden which might react differently to impacts of warming through time.

Although water temperature was not selected at station IR as a macrofauna driver, the fact that the AO index was selected as community fluctuation driver at IR could be linked indirectly to the strength of Atlantic intrusions, the extent of penetration towards the head of the fjord and the effects of prevailing wind patterns in the Rijpfjorden area (Fig. 10). Positive AO phases are positively correlated with inflow anomalies of Atlantic Water in the Barents Sea Opening and onto the shelf areas (Armitage et al., 2018). Wind stress has also been shown to be an important forcing variable in the region (Muilwijk et al., 2018; Smedsrud et al., 2022). When easterly and southerly winds predominate, Ekman transport pushes the pack ice further north and away from the northern coast of Svalbard, leading to shelf-break upwelling which results in the protrusion of Atlantic water onto the shelf (Falk-Petersen et al., 2015, but see Randelhoff and Sundfjord, 2018) (Fig. 1b). Interestingly, in the summer of 2014, exceptional amounts of AW/tW were detected in western Svalbard fjords (Bloshkina et al., 2021; Promińska et al., 2017; Tverberg et al., 2019). In contrast, no signs of tAW presence or warm water anomalies were observed in Rijpfjorden. One possible explanation for this seemingly "intermittent" decoupling between the

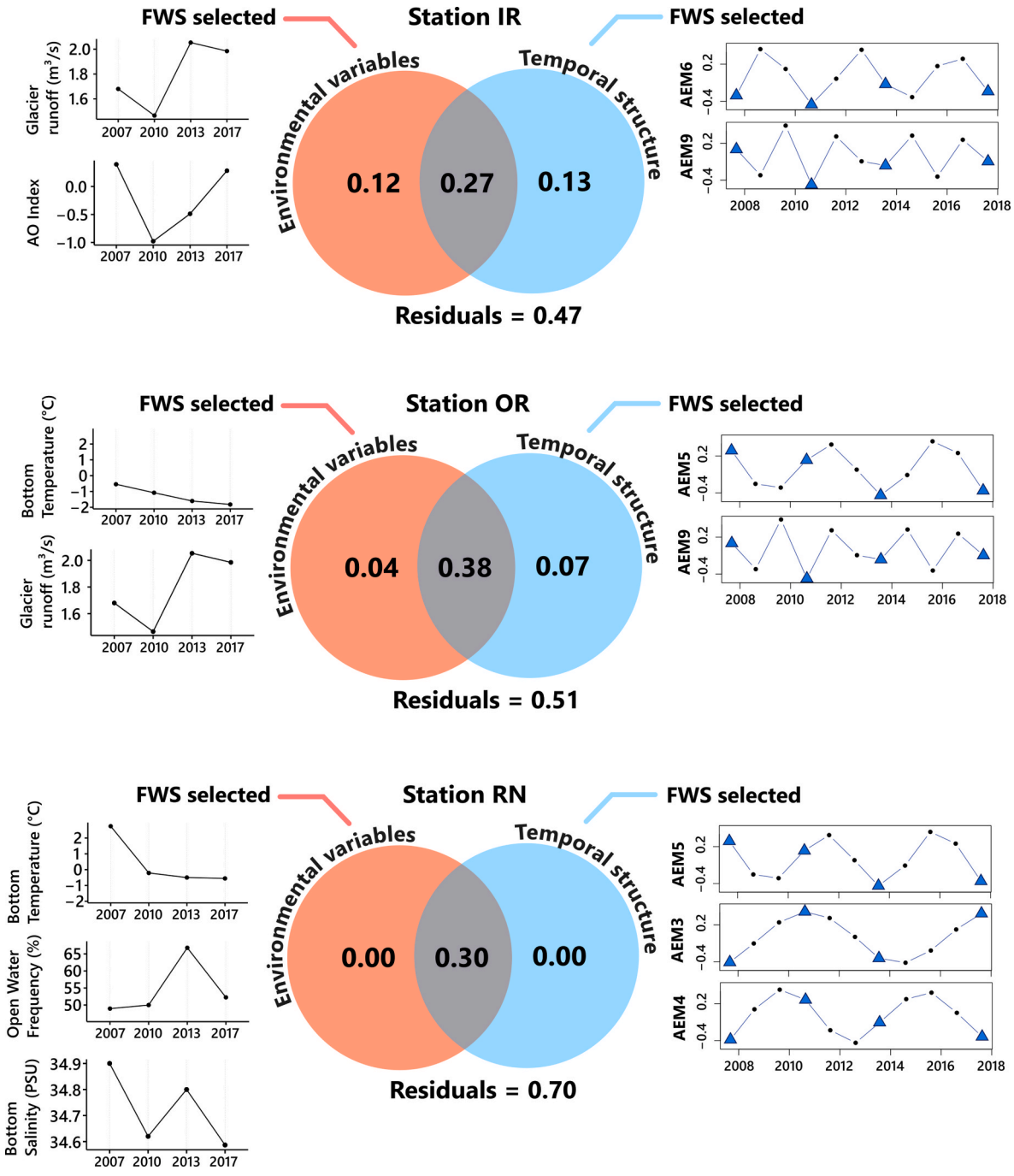

Fig. 10. Venn diagrams of the variation partitioning analysis based on redundancy analysis (RDA) performed with the environmental variables selected after forward selection (pink circle) and the temporal AEMs selected after forward selection (blue circle) at stations IR, Inner Rijpfjorden; OR, Outer Rijpfjorden and RN, Rijpfjorden North, from 2007 to 2017. The numbers in the circles indicate the percentage of variance explained of the macrofauna community (Hellinger transformed) and the circles overlap represents the variance explained by both the environmental variables and the temporal AEMs. Residuals indicate the variance that remains unexplained (either by potential environmental variables not accounted in the time-series or by noise in the data). For each station, the selected environmental variables and the selected AEMs are shown. In the plots from AEMs, blue triangles indicate sampling time of macrofauna events, while the black dots are the dummy variables used to construct the AEMs.

western fjords and the northern fjords could be the local wind patterns prevailing in the north. Nilsen et al., 2021, confirmed that there was a strong correlation between the local wind stress curl pattern over the Yermak Plateau and the seasonal and interannual volume transport anomalies towards the northern shelf of Svalbard. In fact, during summer and autumn of 2014 westerly winds dominated the area (Koenig et al., 2017), pushing the drift ice towards the coast (Lundesgaard et al., 2021) and hampering the lifting of the AW flowing along the continental slope (Svalbard Branch). This stresses the importance to include a northern fjord in monitoring efforts of the archipelagos' fjordic ecosystems, since we cannot rely solely on the processes documented in well studied western fjords to always act as a proxy for northern coastal areas.

The variables selected for OR and RN (bottom temperature, salinity, and open water periods) suggest that the documented SfWWTAs may have played a role in determining macrobenthic structure through time,

perhaps inducing thermal stress to the biological communities and promoting species extirpations in periods with high temperatures and recolonizations in periods with low temperatures. However, other processes and factors such as primary production, food availability, and metabolic demands, which were not covered in this study and that can co-vary with water temperature, could play an important role here. Quantification of food supply and organic matter could be consequently of significance for benthic time-series, as responses might range from community level to species level. For instance, growth rates in Arctic cockles in this fjord indicated that food quality and availability were more important than temperature in initiating growth line depositions (Ambrose et al., 2012).

MHVs have been reported to be as strong in the Arctic Ocean and sub-Arctic seas as in other ocean basins, and their annual intensity has increased in strength during the first two decades of the 21st century compared to 1982–2000 (Huang et al., 2021). Such trends have been reported for the Fram Strait, the Bering Sea, the Siberian Arctic Seas and the Barents Sea (Beszczynska-Möller et al., 2012; Carvalho et al., 2021; Golubeva et al., 2021; Mohamed et al., 2022). In our study, we find evidence that potential MHWs recorded in the form of SfWWTAs and AW-like (tAW) intrusions into Rijpfjorden led to changes in macrofauna communities. Interestingly, this response was clear after the heat wave of 2006, but less drastic changes were observed in later SfWWTAs. Further measurements from the mooring in Rijpfjorden recorded an important SfWWTA extending throughout most part of 2018, indicating a much longer anomaly of warm water than in any of the previous years (Fig. 2a). Mesocosm experiments exposing coastal macrofaunal communities to heatwaves have showcased differential responses to single or sequential MHWs at the community level, with a high response in the sessile/infaunal fraction (Pansch et al., 2018). Diverging responses to episodic versus chronic stress may be due to phenological and functional shifts, while acclimation and post-disturbance biotic interactions could also play important roles (Pansch et al., 2018). Some of these mechanisms might be behind the succession of the communities observed in our study. Other studies have reported unexpected resilience of coral reefs against successive MHWs, where despite high mortality rates during the first onset of disturbance events, they lessened over time despite persistent temperature anomaly periods, suggesting that coral communities could adapt to these new warming conditions (Fox et al., 2021). Moreover, a time series assessing the disturbance impacts of climate driven ice-scouring in shallow zoobenthos from Antarctic waters reported surprising short recovery times (within 10 years) to initial conditions prior to high detrimental impact periods, suggesting that typically considered sensitive cold-water communities seem to be more resilient and recover faster than previously thought in polar environments (Zwerschke et al., 2021). From this, the question arises as to whether the heatwaves documented between 2006 and 2017 in Rijpfjorden have conditioned macrobenthic communities to withstand the thermal stress associated with the last warming event of 2018, or, on the contrary, if a large extirpation event took place once again as in 2006.

5. Conclusions

We found strong evidence that Atlantic intrusions into Rijpfjorden, in the form of SfWWTAs and potential MHWs, led to macrobenthic fluctuations observed in the present intermittent time series (i.e. extirpations followed by recovery periods and posterior re-assembling in different directions at different parts of the fjord axis). In general, macrobenthic communities of this high Arctic fjord appeared to be somewhat resilient to these disturbance events, with recovery periods of up to 4 years (2006–2010). Macrofauna diversity was especially more stable at the inner silled basin, suggesting a certain isolation from strong environmental fluctuations outside the fjord (despite strong variations in community abundances). However, a re-structuring in species composition took place after the recovery in abundance and species richness in 2010. This was mainly attributed to newly dominating taxa from that year onwards at the outer part of the fjord.

Stronger and more frequent Atlantic intrusions plus local manifestations of climate change could lead macrobenthic communities from northern fjords to resemble those of western Svalbard today, which are more exposed to the effects of warm water advections from the shelf areas. There is a possibility that with more drastic disturbance events the communities in the innermost locations, partially protected by the sill, could reach a tipping point despite their recovery capabilities, where they could lose their unique characteristics. This could potentially alter ecosystem services such as carbon sequestration or biogeochemical processes within the fjord, with unknown consequences to the whole fjordic ecosystem, and could put these cold-water refugia at stake. Rijpfjorden, therefore, should be regarded as a model for a cold-water high-Arctic coastal system in transition impacted by periodical warming events.

CRediT author statement

Èric Jordà Molina: Fromal Analysis, Visualization, Data Curation, Writing - Original Draft, Writing - Review & Editing **Paul E. Renaud:** Conceptualization, Investigation, Resources, Writing - Review & Editing, Supervision **Marc J. Silberberger:** Formal Analysis, Visualization, Writing - Review & Editing **Arunima Sen:** Writing - Review & Editing, Supervision **Bodil A. Bluhm:** Writing - Review & Editing, Supervision **Michael L. Carroll:** Conceptualization, Investigation, Resources, Writing - Review & Editing **William G. Ambrose:** Conceptualization, Investigation, Resources, Writing - Review & Editing **Finlo Cottier:** Formal Analysis, Resources, Writing - Review & Editing **Henning Reiss:** Supervision, Writing - Review & Editing.

Funding sources

Internal funding from Nord University. MJS was supported by the National Science Centre, Poland (project: CLIMB – grant no 2019/35/D/NZ8/01282). WGA received support from the National Science Foundation (OPP 1936506). MLC was supported by the Research Council of Norway (project numbers 150356-S30 and 228107). Akvaplan-niva, UiT, and UNIS provided additional support. Additional financial support was provided through the Research Council of Norway (The Nansen Legacy, #276730).

Declaration of competing interest

The authors state that they have no competing financial interests or personal relationships that could influence the work reported in this paper.

Data availability

Data will be made available on request.

Acknowledgements

We thank everyone involved in the sampling and processing of samples at the labs from Akvaplan-Niva, and students Matilda Selina Smollny and Soheyla Anjomipoor (Nord University). We thank Nick Hughes from the Norwegian Ice Service (cryo.met) for providing the sea ice cover files and Jack Kohler from the Norwegian Polar Institute (NPI) for providing the glacier runoff simulations from the areas around Rijpbreen. We thank PhD student Cesc Gordó Vilaseca from Nord University for valuable discussions. William G. Ambrose Jr. is now an employee of the US NSF; however any opinions, findings, and conclusions or recommendations expressed in this material are those of William G. Ambrose Jr. and his co-authors, and do not necessarily reflect the views of the US NSF.

Appendix A. Supplementary data

Supplementary data to this article can be found online at https://doi.org/10.1016/j.marenvres.2023.106046.

References

Ambrose, W.G., Carroll, M.L., Greenacre, M., Thorrold, S.R., McMahon, K.W., 2006. Variation in Serripes groenlandicus (Bivalvia) growth in a Norwegian high-Arctic fjord: evidence for local- and large-scale climatic forcing. Global Change Biol. 12 (9), 1595–1607. https://doi.org/10.1111/j.1365-2486.2006.01181.x.

Ambrose, W.G., Renaud, P.E., Locke, W.L., Cottier, F.R., Berge, J., Carroll, M.L., Levin, B., Ryan, S., 2012. Growth line deposition and variability in growth of two circumpolar bivalves (Serripes groenlandicus, and Clinocardium ciliatum). Polar Biol. 35 (3), 345–354. https://doi.org/10.1007/s00300-011-1080-4.

Armitage, T.W.K., Bacon, S., Kwok, R., 2018. Arctic Sea level and surface circulation response to the arctic oscillation. Geophys. Res. Lett. 45 (13), 6576–6584. https://doi.org/10.1029/2018GL078386.

Athanase, M., Provost, C., Pérez-Hernández, M.D., Sennéchael, N., Bertosio, C., Artana, C., Garric, G., Lellouche, J.-M., 2020. Atlantic water modification north of svalbard in the mercator physical system from 2007 to 2020. J. Geophys. Res.: Oceans 125 (10), e2020JC016463. https://doi.org/10.1029/2020JC016463.

Beszczynska-Möller, A., Fahrbach, E., Schauer, U., Hansen, E., 2012. Variability in Atlantic water temperature and transport at the entrance to the Arctic Ocean, 1997–2010. ICES (Int. Counc. Explor. Sea) J. Mar. Sci. 69 (5), 852–863. https://doi.org/10.1093/icesjms/fss056.

Blanchet, F.G., Legendre, P., Borcard, D., 2008. Forward selection of explanatory variables. Ecology 89 (9), 2623–2632. https://doi.org/10.1890/07-0986.1.

Bloshkina, E. v, Pavlov, A.K., Filchuk, K., 2021. Warming of atlantic water in three West Spitsbergen fjords : recent patterns and century-long trends. Polar Res. 1, 1–11. https://doi.org/10.33265/polar.v40.5392.

Bluhm, B.A., Janout, M.A., Danielson, S.L., Ellingsen, I., Gavrilo, M., Grebmeier, J.M., Hopcroft, R.R., Iken, K.B., Ingvaldsen, R.B., Jørgensen, L.L., Kosobokova, K.N., Kwok, R., Polyakov, I.v., Renaud, P.E., Carmack, E.C., 2020. The pan-arctic continental slope: sharp gradients of physical processes affect pelagic and benthic ecosystems. Front. Mar. Sci. 7 (November), 1–25. https://doi.org/10.3389/fmars.2020.544386.

Borcard, D., Legendre, P., Drapeau, P., 1992. Partialling out the spatial component of ecological variation. Ecology 73 (3), 1045–1055. https://doi.org/10.2307/1940179.

Bourgeois, S., Archambault, P., Witte, U., 2017. Organic matter remineralization in marine sediments: a Pan-Arctic synthesis. Global Biogeochem. Cycles 31 (1), 190–213. https://doi.org/10.1002/2016GB005378.

Carroll, M.L., Ambrose, W.G., 2012. Benthic infaunal community variability on the northern Svalbard shelf. Polar Biol. 35 (8), 1259–1272. https://doi.org/10.1007/s00300-012-1171-x.

Carroll, M.L., Ambrose, W.G., Levin, B.S., Locke, V.W.L., Henkes, G.A., Hop, H., Renaud, P.E., 2011. Pan-Svalbard growth rate variability and environmental regulation in the Arctic bivalve Serripes groenlandicus. J. Mar. Syst. 88 (2), 239–251. https://doi.org/10.1016/j.jmarsys.2011.04.010.

Carvalho, K.S., Smith, T.E., Wang, S., 2021. Bering Sea marine heatwaves: patterns, trends and connections with the Arctic. J. Hydrol. 600, 126462 https://doi.org/10.1016/j.jhydrol.2021.126462.

Cottier, F., Skogseth, R., David, D., de Rovere, F., Vogedes, D., Daase, M., Berge, J., 2022. Temperature and salinity time series in svalbard fjords–'Integrated marine observatory partnership (iMOP II).' in SESS report 2021 - the state of environmental science in svalbard - an annual report. In: Svalbard Integrated Arctic Earth Observing System, pp. 26–36. https://doi.org/10.5281/zenodo.5751717.

Csapó, H.K., Grabowski, M., Węsławski, J.M., 2021. Coming home-Boreal ecosystem claims Atlantic sector of the Arctic. Sci. Total Environ. 771, 144817 https://doi.org/10.1016/j.scitotenv.2020.144817.

Dahlke, S., Hughes, N.E., Wagner, P.M., Gerland, S., Wawrzyniak, T., Ivanov, B., Maturilli, M., 2020. The observed recent surface air temperature development across Svalbard and concurring footprints in local sea ice cover. Int. J. Climatol. 40 (12), 5246–5265. https://doi.org/10.1002/joc.6517.

Dalpadado, P., Ingvaldsen, R.B., Stige, L.C., Bogstad, B., Knutsen, T., Ottersen, G., Ellertsen, B., 2012. Climate effects on Barents Sea ecosystem dynamics. ICES (Int. Counc. Explor. Sea) J. Mar. Sci. 69 (7), 1303–1316. https://doi.org/10.1093/icesjms/fss063.

Dolbeth, M., Babe, O., Costa, D.A., Mucha, A.P., Cardoso, P.G., Arenas, F., 2021. Benthic estuarine communities' contribution to bioturbation under the experimental effect of marine heatwaves. Sci. Rep. 11 (1), 1–11. https://doi.org/10.1038/s41598-021-90720-7.

Dray, S., Bauman, D., Blanchet, G., Borcard, D., Clappe, S., Guenard, G., Jombart, T., Larocque, G., Legendre, P., Madi, N., Wagner, H.H., 2021. Adespatial: multivariate multiscale spatial analysis. R package version 0.3-14. https://CRAN.R-project.org/package=adespatial.

Ehrnsten, E., Norkko, A., Müller-Karulis, B., Gustafsson, E., Gustafsson, B.G., 2020. The meagre future of benthic fauna in a coastal sea—benthic responses to recovery from eutrophication in a changing climate. Global Change Biol. 26 (4), 2235–2250. https://doi.org/10.1111/gcb.15014.

Falk-Petersen, S., Pavlov, V., Berge, J., Cottier, F., Kovacs, K.M., Lydersen, C., 2015. At the rainbow's end: high productivity fueled by winter upwelling along an Arctic shelf. Polar Biol. 38 (1), 5–11. https://doi.org/10.1007/s00300-014-1482-1.

Faust, J.C., Knies, J., 2019. Organic matter sources in north atlantic fjord sediments. G-cubed 20 (6), 2872–2885. https://doi.org/10.1029/2019GC008382.

Fossheim, M., Primicerio, R., Johannesen, E., Ingvaldsen, R.B., Aschan, M.M., Dolgov, A. v., 2015. Recent warming leads to a rapid borealization of fish communities in the Arctic. Nat. Clim. Change 5 (7), 673–677. https://doi.org/10.1038/nclimate2647.

Fox, M.D., Cohen, A.L., Rotjan, R.D., Mangubhai, S., Sandin, S.A., Smith, J.E., Thorrold, S.R., Dissly, L., Mollica, N.R., Obura, D., 2021. Increasing coral reef resilience through successive marine heatwaves. Geophys. Res. Lett. 48 (17), e2021GL094128 https://doi.org/10.1029/2021GL094128.

Garrabou, J., Coma, R., Bensoussan, N., Bally, M., Chevaldonné, P., Cigliano, M., Díaz, D., Harmelin, J.-G., Gambi, M.C., Kersting, D.K., 2009. Mass mortality in Northwestern Mediterranean rocky benthic communities: effects of the 2003 heat wave. Global Change Biol. 15 (5), 1090–1103. https://doi.org/10.1111/j.1365-2486.2008.01823.x.

Garrabou, J., Gómez-Gras, D., Medrano, A., Cerrano, C., Ponti, M., Schlegel, R., Bensoussan, N., Turicchia, E., Sini, M., Gerovasileiou, V., Teixido, N., Mirasole, A., Tamburello, L., Cebrian, E., Rilov, G., Ledoux, J.-B., Souissi, J. ben, Khamassi, F., Ghanem, R., et al., 2022. Marine heatwaves drive recurrent mass mortalities in the Mediterranean Sea. Global Change Biol. 28 (19), 5708–5725. https://doi.org/10.1111/gcb.16301.

GEBCO Compilation Group, 2022. GEBCO_2022 Grid. https://doi.org/10.5285/e0f0bb80-ab44-2739-e053-6c86abc0289c.

Golubeva, E., Kraineva, M., Platov, G., Iakshina, D., Tarkhanova, M., 2021. Marine heatwaves in Siberian Arctic seas and adjacent region. Rem. Sens. 13 (21), 4436. https://doi.org/10.3390/rs13214436.

Górska, B., Gromisz, S., Legeżyńska, J., Soltwedel, T., Włodarska-Kowalczuk, M., 2022. Macrobenthic diversity response to the atlantification of the Arctic Ocean (Fram Strait, 79° N)–A taxonomic and functional trait approach. Ecol. Indicat. 144, 109464 https://doi.org/10.1016/j.ecolind.2022.109464.

Griffiths, J.R., Kadin, M., Nascimento, F.J.A., Tamelander, T., Törnroos, A., Bonaglia, S., Bonsdorff, E., Brüchert, V., Gårdmark, A., Järnström, M., Kotta, J., Lindegren, M., Nordström, M.C., Norkko, A., Olsson, J., Weigel, B., Žydelis, R., Blenckner, T., Niiranen, S., Winder, M., 2017. The importance of benthic–pelagic coupling for marine ecosystem functioning in a changing world. Global Change Biol. 23 (6), 2179–2196. https://doi.org/10.1111/gcb.13642.

Grzelak, K., 2015. Structural and Functional Diversity of Nematoda at the Arctic Deep-Sea Long Term Observatory HAUSGARTEN (Fram Strait) (PhD thesis). Institute of Oceanology Polish Academy of Sciences, Sopot, p. 206.

Hobday, A.J., Alexander, L. v, Perkins, S.E., Smale, D.A., Straub, S.C., Oliver, E.C.J., Benthuysen, J.A., Burrows, M.T., Donat, M.G., Feng, M., 2016. A hierarchical approach to defining marine heatwaves. Prog. Oceanogr. 141, 227–238. https://doi.org/10.1016/j.pocean.2015.12.014.

Holte, B., Gulliksen, B., 1998. Common macrofaunal dominant species in the sediments of some north Norwegian and Svalbard glacial fjords. Polar Biol. 19 (6), 375–382. https://doi.org/10.1007/s003000050262.

Hop, H., Assmy, P., Wold, A., Sundfjord, A., Daase, M., Duarte, P., Kwasniewski, S., Gluchowska, M., Wiktor, J.M., Tatarek, A., Wiktor, J., Kristiansen, S., Fransson, A., Chierici, M., Vihtakari, M., 2019. Pelagic ecosystem characteristics across the atlantic water boundary current from Rijpfjorden, Svalbard, to the Arctic ocean during summer (2010-2014). Front. Mar. Sci. 6 (APR), 1–21. https://doi.org/10.3389/fmars.2019.00181.

Hoste, E., Vanhove, S., Schewe, I., Soltwedel, T., Vanreusel, A., 2007. Spatial and temporal variations in deep-sea meiofauna assemblages in the marginal ice zone of the Arctic Ocean. Deep Sea Res. Oceanogr. Res. Pap. 54 (1), 109–129. https://doi.org/10.1016/j.dsr.2006.09.007.

Huang, B., Wang, Z., Yin, X., Arguez, A., Graham, G., Liu, C., Smith, T., Zhang, H., 2021. Prolonged marine heatwaves in the Arctic: 1982– 2020. Geophys. Res. Lett. 48 (24), e2021GL095590 https://doi.org/10.1029/2021GL095590.

Ingvaldsen, R.B., Assmann, K.M., Primicerio, R., Fossheim, M., Polyakov, I. v, Dolgov, A. v., 2021. Physical manifestations and ecological implications of Arctic Atlantification. Nat. Rev. Earth Environ. 2 (12), 874–889. https://doi.org/10.1038/s43017-021-00228-x.

Isaksen, K., Nordli, Ø., Ivanov, B., Køltzow, M.A.Ø., Aaboe, S., Gjelten, H.M., Mezghani, A., Eastwood, S., Førland, E., Benestad, R.E., 2022. Exceptional warming over the Barents area. Sci. Rep. 12 (1), 1–18. https://doi.org/10.1038/s41598-022-13568-5.

Johansson, A.M., Malnes, E., Gerland, S., Cristea, A., Doulgeris, A.P., Divine, D. v, Pavlova, O., Lauknes, T.R., 2020. Consistent ice and open water classification combining historical synthetic aperture radar satellite images from ERS-1/2, Envisat ASAR, RADARSAT-2 and Sentinel-1A/B. Ann. Glaciol. 61 (82), 40–50. https://doi.org/10.1017/aog.2019.52.

Jordà Molina, È., Silberberger, M.J., Kokarev, V., Reiss, H., 2019. Environmental drivers of benthic community structure in a deep sub-arctic fjord system. Estuar. Coast Shelf Sci. 225 (May), 106239 https://doi.org/10.1016/j.ecss.2019.05.021.

Kauppi, L., Göbeler, N., Norkko, J., Norkko, A., Romero-Ramirez, A., Bernard, G., 2023. Changes in macrofauna bioturbation during repeated heatwaves mediate changes in biogeochemical cycling of nutrients. Front. Mar. Sci. 9 https://doi.org/10.3389/fmars.2022.1070377.

Kędra, M., Włodarska-Kowalczuk, M., Wesławski, J.M., 2010. Decadal change in macrobenthic soft-bottom community structure in a high Arctic fjord (Kongsfjorden, Svalbard). Polar Biol. 33 (1), 1–11. https://doi.org/10.1007/s00300-009-0679-1.

Koenig, Z., Provost, C., Villacieros-Robineau, N., Sennéchael, N., Meyer, A., Lellouche, J.-M., Garric, G., 2017. Atlantic waters inflow north of Svalbard: insights from IAOOS observations and Mercator Ocean global operational system during N-ICE2015. J. Geophys. Res.: Oceans 122 (2), 1254–1273. https://doi.org/10.1002/2016JC012424.

Kolås, E.H., Koenig, Z., Fer, I., Nilsen, F., Marnela, M., 2020. Structure and transport of atlantic water north of svalbard from observations in summer and fall 2018. J. Geophys. Res.: Oceans 125 (9). https://doi.org/10.1029/2020JC016174.
Kortsch, S., Primicerio, R., Beuchel, F., Renaud, P.E., Rodrigues, J., Lønne, O.J., Gulliksen, B., 2012. Climate-driven regime shifts in Arctic marine benthos. Proc. Natl. Acad. Sci. USA 109 (35), 14052–14057. https://doi.org/10.1073/pnas.1207509109.
Kraft, A., Nöthig, E.M., Bauerfeind, E., Wildish, D.J., Pohle, G.W., Bathmann, U.V., Beszczynska-Möller, A., Klages, M., 2013. First evidence of reproductive success in a southern invader indicates possible community shifts among Arctic zooplankton. Mar. Ecol. Prog. Ser. 493, 291–296. https://doi.org/10.3354/meps10507.
Kröncke, I., Dippner, J.W., Heyen, H., Zeiss, B., 1998. Long-term changes in macrofaunal communities off Norderney (East Frisia, Germany) in relation to climate variability. Mar. Ecol. Prog. Ser. 167, 25–36. https://doi.org/10.3354/meps167025.
Larkin, K., Ruhl, H.A., Bagley, P., Benn, A., Bett, B.J., Billet, D.S.M., Boetius, A., Chevaldonné, P., Colaco, A., Copley, J., Danovaro, R., Escobar-Briones, E., Glover, A., Gooday, A.J., Hughes, J.A., Kalogeropoulou, V., Kelly-Gerreyn, B.A., Kitazato, H., Klages, M., Lampadariou, N., Lejeusne, C., Perez, T., Priede, I.G., Rogers, A., Sarradin, P.M., Sarrazin, J., Soltwedel, T., Soto, E.H., Thatje, S., Tselepides, A., Tyler, P.A., van den Hove, S., Vanreusel, A., Wenzhöfer, F., 2010. Benthic biology time-series in the deep sea: indicators of change , OceanObs'09 - community white paper. https://doi.org/10.5270/oceanobs09.cwp.52.
Legendre, P., 2019. A temporal beta-diversity index to identify sites that have changed in exceptional ways in space–time surveys. Ecol. Evol. 9 (6), 3500–3514. https://doi.org/10.1002/ece3.4984.
Legendre, P., Borcard, D., 2018. Box–Cox-chord transformations for community composition data prior to beta diversity analysis. Ecography 41 (11), 1820–1824. https://doi.org/10.1111/ecog.03498.
Legendre, P., de Cáceres, M., 2013. Beta diversity as the variance of community data: dissimilarity coefficients and partitioning. Ecol. Lett. 16 (8), 951–963. https://doi.org/10.1111/ele.12141.
Legendre, P., Gallagher, E.D., 2001. Ecologically meaningful transformations for ordination of species data. Oecologia 129 (2), 271–280. https://doi.org/10.1007/s004420100716.
Legendre, P., Gauthier, O., 2014. Statistical methods for temporal and space-time analysis of community composition data. Proc. Biol. Sci. 281 (1778) https://doi.org/10.1098/rspb.2013.2728.
Leu, E., Søreide, J.E., Hessen, D.O., Falk-Petersen, S., Berge, J., 2011. Consequences of changing sea-ice cover for primary and secondary producers in the European Arctic shelf seas: timing, quantity, and quality. Prog. Oceanogr. 90 (1), 18–32. https://doi.org/10.1016/j.pocean.2011.02.004.
Lundesgaard, Ø., Sundfjord, A., Renner, A.H., 2021. Drivers of interannual sea ice concentration variability in the Atlantic water inflow region north of Svalbard. J. Geophys. Res. 126 (4), e2020JC016522 https://doi.org/10.1029/2020JC016522.
McMahon, K.W., Ambrose, W.G., Johnson, B.J., Sun, M.-Y., Lopez, G.R., Clough, L.M., Carroll, M.L., 2006. Benthic community response to ice algae and phytoplankton in Ny Ålesund, Svalbard. Mar. Ecol. Prog. Ser. 310, 1–14. https://doi.org/10.3354/meps310001.
Mohamed, B., Nilsen, F., Skogseth, R., 2022. Marine Heatwaves Characteristics in the Barents Sea based on high resolution satellite data (1982–2020). Front. Mar. Sci. 13, 4436. https://doi.org/10.3389/fmars.2022.82164.
Molis, M., Beuchel, F., Laudien, J., Włodarska-Kowalczuk, M., Buschbaum, C., 2019. In: Hop, Svalbard (H., Wiencke, C. (Eds.), Ecological Drivers of and Responses by Arctic Benthic Communities, with an Emphasis on Kongsfjorden, Svalbard BT - the Ecosystem of Kongsfjorden, 423–481. Springer International Publishing. https://doi.org/10.1007/978-3-319-46425-1_11.
Muilwijk, M., Smedsrud, L.H., Ilicak, M., Drange, H., 2018. Atlantic Water heat transport variability in the 20th century Arctic Ocean from a global ocean model and observations. J. Geophys. Res.: Oceans 123 (11), 8159–8179. https://doi.org/10.1029/2018JC014327.
Nelson, D.W., Sommers, L.E., 1996. Total carbon, organic carbon, and organic matter. Methods Soil Anal.: Part 3 Chem. Methods 5, 961–1010. https://doi.org/10.2136/sssabookser5.3.c34.
Nilsen, F., Ersdal, E.A., Skogseth, R., 2021. Wind-driven variability in the spitsbergen polar current and the svalbard branch across the Yermak Plateau. J. Geophys. Res.: Oceans 126 (9), e2020JC016734. https://doi.org/10.1029/2020JC016734.
Oksanen, J., Blanchet, F.G., Friendly, M., Kindt, R., Legendre, P., McGlinn, D., Minchin, P.R., O'Hara, R.B., Simpson, G.L., Solymos, P., Stevens, M.H.H., Szoecs, E., Wagner, H., 2020. vegan: Community Ecology Package. R package version 2.5-7. https://CRAN.R-project.org/package=vegan.
Olden, J.D., Poff, N.L., 2003. Redundancy and the choice of hydrologic indices for characterizing streamflow regimes. River Res. Appl. 19 (2), 101–121. https://doi.org/10.1002/rra.700.
Onarheim, I.H., Smedsrud, L.H., Ingvaldsen, R.B., Nilsen, F., 2014. Loss of sea ice during winter north of Svalbard. Tellus A: Dynam. Meteorol. Oceanogr. 66 (1) https://doi.org/10.3402/tellusa.v66.23933.
Pansch, C., Scotti, M., Barboza, F.R., Al-Janabi, B., Brakel, J., Briski, E., Bucholz, B., Franz, M., Ito, M., Paiva, F., Saha, M., Sawall, Y., Weinberger, F., Wahl, M., 2018. Heat waves and their significance for a temperate benthic community: a near-natural experimental approach. Global Change Biol. 24 (9), 4357–4367. https://doi.org/10.1111/gcb.14282.
Polyakov, I.v., Alkire, M.B., Bluhm, B.A., Brown, K.A., Carmack, E.C., Chierici, M., Danielson, S.L., Ellingsen, I., Ershova, E.A., Gårdfeldt, K., Ingvaldsen, R.B., Pnyushkov, A.v., Slagstad, D., Wassmann, P., 2020. Borealization of the Arctic Ocean in response to anomalous advection from sub-arctic seas. Front. Mar. Sci. 7 (July) https://doi.org/10.3389/fmars.2020.00491.
Promińska, A., Cisek, M., Walczowski, W., 2017. Kongsfjorden and Hornsund hydrography – comparative study based on a multiyear survey in fjords of west Spitsbergen. Oceanologia 59 (4), 397–412. https://doi.org/10.1016/j.oceano.2017.07.003.
QGIS.org, 2022. QGIS Geographic Information System. QGIS Association. http://www.qgis.org.
Ramondenc, S., Nöthig, E.M., Hufnagel, L., Bauerfeind, E., Busch, K., Knüppel, N., Kraft, A., Schröter, F., Seifert, M., Iversen, M.H., 2002. Effects of Atlantification and changing sea-ice dynamics on zooplankton community structure and carbon flux between 2000 and 2016 in the eastern Fram Strait. Limnol. Oceanogr. https://doi.org/10.1002/lno.12192.
Randelhoff, A., Sundfjord, A., 2018. Short commentary on marine productivity at Arctic shelf breaks: upwelling, advection and vertical mixing. Ocean Sci. 14 (2), 293–300. https://doi.org/10.5194/os-14-293-2018.
Rantanen, M., Karpechko, A.Y., Lipponen, A., Nordling, K., Hyvärinen, O., Ruosteenoja, K., Vihma, T., Laaksonen, A., 2022. The Arctic has warmed nearly four times faster than the globe since 1979. Commun. Earth Environ. 3 (1), 1–10. https://doi.org/10.1038/s43247-022-00498-3.
Renaud, P.E., Morata, N., Carroll, M.L., Denisenko, S.G., Reigstad, M., 2008. Pelagic-benthic coupling in the western Barents Sea: processes and time scales. Deep-Sea Res. Part II Top. Stud. Oceanogr. 55 (20–21), 2372–2380. https://doi.org/10.1016/j.dsr2.2008.05.017.
Renaud, P.E., Sejr, M.K., Bluhm, B.A., Sirenko, B., Ellingsen, I.H., 2015. The future of Arctic benthos: expansion, invasion, and biodiversity. Prog. Oceanogr. 139, 244–257. https://doi.org/10.1016/j.pocean.2015.07.007.
Renaud, P.E., Wallhead, P., Kotta, J., Włodarska-Kowalczuk, M., Bellerby, R.G.J., Rätsep, M., Slagstad, D., Kukliński, P., 2019. Arctic sensitivity? Suitable habitat for benthic taxa is surprisingly robust to climate change. Front. Mar. Sci. 6, 538. https://doi.org/10.3389/fmars.2019.00538.
Renaud, P.E., Włodarska-Kowalczuk, M., Trannum, H., Holte, B., Węsławski, J.M., Cochrane, S., Dahle, S., Gulliksen, B., 2007. Multidecadal stability of benthic community structure in a high-Arctic glacial fjord (van Mijenfjord, Spitsbergen). Polar Biol. 30 (3), 295–305. https://doi.org/10.1007/s00300-006-0183-9.
Rigor, I.G., Wallace, J.M., Colony, R.L., 2002. Response of sea ice to the arctic oscillation. J. Clim. 15 (18), 2648–2663. https://doi.org/10.1175/1520-0442(2002)015<2648:ROSITT>2.0.CO;2.
Santos-Garcia, M., Ganeshram, R.S., Tuerena, R.E., Debyser, M.C.F., Husum, K., Assmy, P., Hop, H., 2022. Nitrate isotope investigations reveal future impacts of climate change on nitrogen inputs and cycling in Arctic fjords: Kongsfjorden and Rijpfjorden (Svalbard). EGUsphere 1–47. https://doi.org/10.5194/egusphere-2022-584.
Serrano, A., de la Torriente, A., Punzón, A., Blanco, M., Bellas, J., Durán-Muñoz, P., Murillo, F.J., Sacau, M., García-Alegre, A., Antolínez, A., Elliott, S., Guerin, L., Vina-Herbón, C., Marra, S., González-Irusta, J.M., 2022. Sentinels of Seabed (SoS) indicator: assessing benthic habitats condition using typical and sensitive species. Ecol. Indicat. 140, 108979 https://doi.org/10.1016/j.ecolind.2022.108979.
Skogseth, R., Ellingsen, P., Berge, J., Cottier, F., Falk-Petersen, S., Ivanov, B., Nilsen, F., Søreide, J., Vader, A., 2019. UNIS Hydrographic Database [Data Set]. Norwegian Polar Institute. https://doi.org/10.21334/unis-hydrography.
Ślubowska, M.A., Koç, N., Rasmussen, T.L., Klitgaard-Kristensen, D., 2005. Changes in the flow of Atlantic water into the Arctic Ocean since the last deglaciation: evidence from the northern Svalbard continental margin, 80°N. Paleoceanography 20 (4). https://doi.org/10.1029/2005PA001141.
Smedsrud, L.H., Muilwijk, M., Brakstad, A., Madonna, E., Lauvset, S.K., Spensberger, C., Born, A., Eldevik, T., Drange, H., Jeansson, E., Li, C., Olsen, A., Skagseth, Ø., Slater, D.A., Straneo, F., Våge, K., Årthun, M., 2022. Nordic Seas heat loss, Atlantic inflow, and Arctic sea ice cover over the last century. Rev. Geophys. 60 (1), e2020RG000725 https://doi.org/10.1029/2020RG000725.
Smith, R.W., Bianchi, T.S., Allison, M., Savage, C., Galy, V., 2015. High rates of organic carbon burial in fjord sediments globally. Nat. Geosci. 8 (6), 450–453. https://doi.org/10.1038/NGEO2421.
Solan, M., Ward, E.R., Wood, C.L., Reed, A.J., Grange, L.J., Godbold, J.A., 2020. Climate-driven benthic invertebrate activity and biogeochemical functioning across the Barents Sea polar front. Philos. Trans. R. Soc. A 378 (2181), 20190365. https://doi.org/10.1098/rsta.2019.0365.
Soltwedel, T., Bauerfeind, E., Bergmann, M., Bracher, A., Budaeva, N., Busch, K., Cherkasheva, A., Fahl, K., Grzelak, K., Hasemann, C., Jacob, M., Kraft, A., Lalande, C., Metfies, K., Nöthig, E., Meyer, K., Quéric, N., Schewe, I., Włodarska-Kowalczuk, M., Klages, M., 2016. Natural variability or anthropogenically-induced variation? Insights from 15 years of multidisciplinary observations at the arctic marine LTER site HAUSGARTEN. Ecol. Indicat. 65, 89–102. https://doi.org/10.1016/j.ecolind.2015.10.001.
Tatsumi, S., 2022. Ecopart: Partitioning the Temporal Changes in Beta Diversity into Extinction and Colonization Components. R package version 0.2.0.
Tatsumi, S., Iritani, R., Cadotte, M.W., 2021. Temporal changes in spatial variation: partitioning the extinction and colonisation components of beta diversity. Ecol. Lett. 24 (5), 1063–1072. https://doi.org/10.1111/ele.13720.
Tatsumi, S., Strengbom, J., Čugunovs, M., Kouki, J., 2020. Partitioning the colonization and extinction components of beta diversity across disturbance gradients. Ecology 101 (12), e03183. https://doi.org/10.1002/ecy.3183.
Torsvik, T., Albretsen, J., Sundfjord, A., Kohler, J., Sandvik, A., Skarðhamar, J., 2019. Impact of tidewater glacier retreat on the fjord system: modeling present and future circulation in Kongsfjorden. Svalbard. Estuar. Coast Shelf Sci. https://doi.org/10.1016/j.ecss.2019.02.005.

Trannum, H. C., Pedersen, K. B., Renaud, P. E., Christensen, G. N., & Evenset, A. (n.d.). Recolonisation and Recovery of an Arctic Benthic Community Subject to Mine-Tailings Deposits. Available at SSRN 4089557.

Tsubouchi, T., Våge, K., Hansen, B., Larsen, K.M.H., Østerhus, S., Johnson, C., Jónsson, S., Valdimarsson, H., 2021. Increased ocean heat transport into the Nordic seas and Arctic Ocean over the period 1993–2016. Nat. Clim. Change 11 (1), 21–26. https://doi.org/10.1038/s41558-020-00941-3.

Tverberg, V., Skogseth, R., Cottier, F., Sundfjord, A., Walczowski, W., Inall, M.E., Falck, E., Pavlova, O., Nilsen, F., 2019. In: Hop, Svalbard (H., Wiencke, C. (Eds.), The Kongsfjorden Transect: Seasonal and Inter-annual Variability in Hydrography BT - the Ecosystem of Kongsfjorden. Springer International Publishing, pp. 49–104. https://doi.org/10.1007/978-3-319-46425-1_3.

Udalov, A., Chikina, M., Chava, A., Vedenin, A., Shchuka, S., Mokievsky, V., 2021. Patterns of benthic communities in Arctic fjords (Novaya Zemlya archipelago, Kara Sea): resilience vs. fragility. Front. Ecol. Evol. 9 (November), 1–18. https://doi.org/10.3389/fevo.2021.777006.

van Pelt, W., Pohjola, V., Pettersson, R., Marchenko, S., Kohler, J., Luks, B., Hagen, J.O., Schuler, T. v, Dunse, T., Noël, B., Reijmer, C., 2019. A long-term dataset of climatic mass balance, snow conditions, and runoff in Svalbard (1957–2018). Cryosphere 13 (9), 2259–2280. https://doi.org/10.5194/tc-13-2259-2019.

Vihtakari, M., 2020. PlotSvalbard: PlotSvalbard - plot research data from svalbard on maps. R package version 0.9.2. https://github.com/MikkoVihtakari/PlotSvalbard.

Wallace, M.I., Cottier, F.R., Berge, J., Tarling, G.A., Griffiths, C., Brierley, A.S., 2010. Comparison of zooplankton vertical migration in an ice-free and a seasonally ice-covered Arctic fjord: an insight into the influence of sea ice cover on zooplankton behavior. Limnol. Oceanogr. 55 (2), 831–845. https://doi.org/10.4319/lo.2009.55.2.0831.

Wang, C., Shi, L., Gerland, S., Granskog, M.A., Renner, A.H.H., Li, Z., Hansen, E., Martma, T., 2013. Spring sea-ice evolution in Rijpfjorden (80° N), Svalbard, from in situ measurements and ice mass-balance buoy (IMB) data. Ann. Glaciol. 54 (62), 253–260. https://doi.org/10.3189/2013AoG62A135.

Wassmann, P., Duarte, C.M., Agustí, S., Sejr, M.K., 2011. Footprints of climate change in the Arctic marine ecosystem. Global Change Biol. 17 (2), 1235–1249. https://doi.org/10.1111/j.1365-2486.2010.02311.x.

Węsławski, J.M., Buchholz, F., Głuchowska, M., Weydmann, A., 2017. Ecosystem maturation follows the warming of the Arctic fjords. Oceanologia 59 (4), 592–602. https://doi.org/10.1016/j.oceano.2017.02.002.

Wesławski, J.M., Kendall, M.A., Włodarska-Kowalczuk, M., Iken, K., Kedra, M., Legezynska, J., Sejr, M.K., 2011. Climate change effects on Arctic fjord and coastal macrobenthic diversity-observations and predictions. Mar. Biodivers. 41 (1), 71–85. https://doi.org/10.1007/s12526-010-0073-9.

Weydmann-Zwolicka, A., Prątnicka, P., Łącka, M., Majaneva, S., Cottier, F., Berge, J., 2021. Zooplankton and sediment fluxes in two contrasting fjords reveal Atlantification of the Arctic. Sci. Total Environ. 773, 145599 https://doi.org/10.1016/j.scitotenv.2021.145599.

Whittaker, R.H., 1972. Evolution and measurement of species diversity. Taxon 21 (2–3), 213–251. https://doi.org/10.2307/1218190.

Whitaker, D., Christman, M., 2014. Clustsig: significant cluster analysis. R package version 1.1. https://CRAN.R-project.org/package=clustsig.

Włodarska-Kowalczuk, M., Mazurkiewicz, M., Górska, B., Michel, L.N., Jankowska, E., Zaborska, A., 2019. Organic carbon origin, benthic faunal consumption, and burial in sediments of Northern Atlantic and Arctic fjords (60–81°N). J. Geophys. Res.: Biogeosciences 124 (12), 3737–3751. https://doi.org/10.1029/2019JG005140.

Włodarska-Kowalczuk, M., Pearson, T.H., 2004. Soft-bottom macrobenthic faunal associations and factors affecting species distributions in an Arctic glacial fjord (Kongsfjord, Spitsbergen). Polar Biol. 27 (3), 155–167. https://doi.org/10.1007/s00300-003-0568-y.

Włodarska-Kowalczuk, M., Pearson, T.H., Kendall, Michael A., 2005. Benthic response to chronic natural physical disturbance by glacial sedimentation in an Arctic fjord. Mar. Ecol. Prog. Ser. 303, 31–41. https://doi.org/10.3354/meps303031.

Włodarska-Kowalczuk, M., Renaud, P.E., Węsławski, J.M., Cochrane, S.K.J., Denisenko, S.G., 2012. Species diversity, functional complexity and rarity in Arctic fjordic versus open shelf benthic systems. Mar. Ecol. Prog. Ser. 463, 73–87. https://doi.org/10.3354/meps09858. Pearson 1980.

Włodarska-Kowalczuk, M., Węsawski, J.M., Kotwicki, L., 1998. Spitsbergen glacial bays macrobenthos - a comparative study. Polar Biol. 20 (1), 66–73. https://doi.org/10.1007/s003000050277.

Wood, S.N., 2011. Fast stable restricted maximum likelihood and marginal likelihood estimation of semiparametric generalized linear models. J. Roy. Stat. Soc. 73 (1), 3–36.

WoRMS Editorial Board, 2022. World register of marine species. Available from. https://www.marinespecies.org. at VLIZ. Accessed 2022-10-12.

Zwerschke, N., Morley, S.A., Peck, L.S., Barnes, D.K.A., 2021. Can Antarctica's shallow zoobenthos 'bounce back' from iceberg scouring impacts driven by climate change? Global Change Biol. 27 (13), 3157–3165. https://doi.org/10.1111/gcb.15617.